The Geological Society of America
Special Paper 428
2007

Transtensional deformation of the western Caribbean–North America plate boundary zone

Robert D. Rogers*
Paul Mann
John A. and Katherine G. Jackson School of Geosciences, The University of Texas at Austin, 4412 Spicewood Springs Road, Building 600, Austin, Texas, 78759-8500, USA

ABSTRACT

Divergence, expressed as the angle between the plate motion vector and the azimuth of a plate margin fault, has been proposed to explain development of contrasting styles of transtensional deformation along transform margins. We present the western North America–Caribbean plate margin as a test of this hypothesis. Here, geologic, earthquake, marine geophysical, and remote sensing data show two distinct structural styles: (1) east-west extension along north-trending rifts normal to the plate margin in the western study area (western Honduras and southern Guatemala); and (2) NNW-SSE transtension along rifts subparallel to the plate margin in the eastern study area (northern Honduras and offshore Honduran borderlands region). Orientations of rifts in each area coincide with the angle of divergence between the GPS-derived plate motion vector and the azimuth of the plate boundary fault, such that the western zone of east-west extension has an angle >10°, while the eastern zone of NNW-SSE extension occurs when the angle of divergence is between 5° and 10°. A narrow transition area in north-central Honduras separates the plate boundary–normal rifts of western Honduras from the plate boundary–parallel rifts to the east.

Faults of the offshore Honduran borderlands extend onshore into the Nombre de Dios range and Aguan Valley of northern Honduras where tectonic geomorphology studies show pervasive oblique-slip faulting with active left-lateral river offsets and active uplift of stream reaches. Offshore, seismic data tied to wells in the Honduran borderlands reveal active submarine faults bounding asymmetric half-grabens filled by middle Miocene clastic wedges with continued deposition to Pliocene-Pleistocene. The north-trending rifts of western Honduras form discontinuous half grabens that cut the late Miocene ignimbrite strata. Plate reconstructions indicate the north-trending rifts of western Honduras developed in response to increased interplate divergence as the western margin of the Caribbean plate shifted from the Jocotan fault to the Polochic fault in the middle Miocene.

Keywords: Honduran borderlands, oblique divergence, geomorphology, Caribbean plate.

*Now at Department of Geology, California State University Stanislaus, 801 West Monte Vista Avenue, Turlock, California 95382, USA; rrogers@geology.csustan.edu.

Rogers, R.D., and Mann, P., 2007, Transtensional deformation of the western Caribbean-North America plate boundary zone, *in* Mann, P., ed., Geologic and tectonic development of the Caribbean plate in northern Central America: Geological Society of America Special Paper 428, p. 37–64, doi: 10.1130/2007.2428(03).

INTRODUCTION

Strain partitioning along plate margins produces complex but characteristic deformation patterns along plate boundary faults. Most previous studies of strain partitioning have come from transpressive regions where convergent plate motion is transformed into components of strike-slip and thrust faulting in either ancient (cf. Teyssier et al., 1995; Jones and Tanner, 1995; Claypool et al., 2002) or active settings (Marshall et al., 2000; Calais et al., 2002; Mann et al., 2002; Meckel et al., 2003). In contrast, there are few examples documented from active transtensional settings where obliquely divergent plate motion is partitioned into coexisting strike-slip and normal components of deformation (Ben-Avraham and Zoback, 1992; Ben-Avraham, 1992).

Key questions for understanding strain partitioning in transtensional settings include (1) how much strain is accommodated by strike-slip faulting versus normal faulting along each plate boundary segment; (2) what controls different styles of coexisting strike-slip and normal faulting along a plate boundary; (3) what controls the transition from one style of transtensional strain partitioning to another and where this occurs; and (4) how successive styles of transtension are superimposed as a plate boundary evolves.

We present the northwestern margin of the Caribbean plate as an example of strain partitioning in a transtensional setting and examine in detail the resulting deformational patterns as observed onshore in Honduras and Guatemala and beneath the adjacent Caribbean Sea (Honduran borderlands). This region is ideal for such a study for several reasons:

1. GPS-based geodesy from DeMets et al. (2000) places firm constraints on the variation of interplate motion and deformational styles across a 3100-km-long segment of the North America–Caribbean plate boundary (Fig. 1).
2. Plate boundary-related normal faults of a variety of orientations and ages are present in northern Central America and in adjacent areas of the Honduran borderlands (Fig. 2).
3. Plate margin faults have known variations in position and orientation that can be tied to quantitative plate reconstructions based on the opening history of the Cayman trough and surrounding plate pairs.

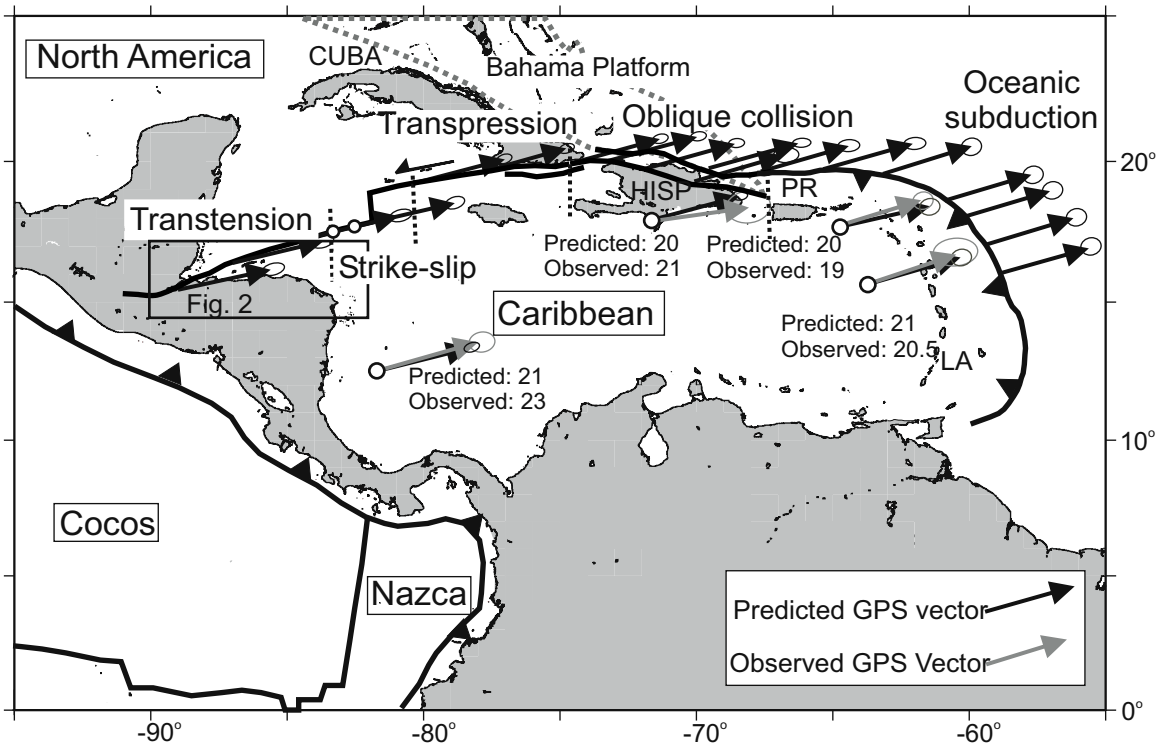

Figure 1. Seismotectonic setting of the Caribbean plate. BR in upper diagram is the Beata Ridge. Line LNR shows the general location and trend of the Lower Nicaraguan Rise, which extends ~1000 km northeastward from the Caribbean coast of Nicaragua toward southern Hispaniola. Open diamonds show locations of GPS sites whose velocities are employed in this study. Filled diamond shows 15°N, 75°W fiducial location employed for the analysis. Area enclosed in rectangle is displayed in Figure 6. All earthquakes above depths of 60 km and with surface- or body-wave magnitudes >3.5 for the period 1963 through 2004 are shown in the lower diagram. AVES, BARA, BARB, CRO1, FSD0/1, JAMA, ROJO, and SANA are site names discussed in text.

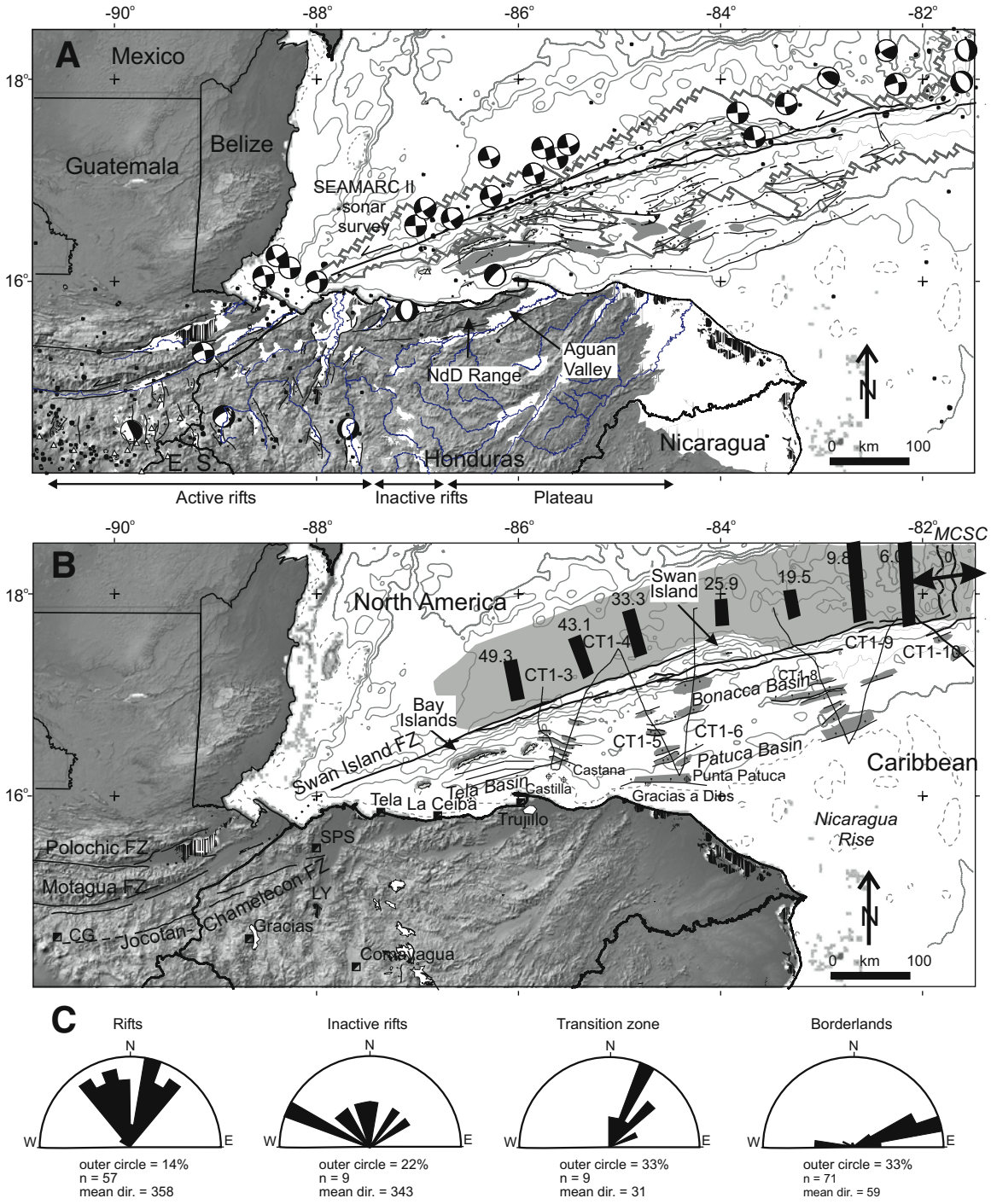

Figure 2. GPS site velocities relative to the North America plate on an oblique Mercator map projected about the best-fitting Caribbean–North America pole of rotation. Numerals by site names give the site rates in millimeters per year. Open arrow indicates motion of site ESTI, where the antenna is mounted on a tall steel tower of questionable stability. The location of GPS site BARA discussed in the text is shown in Figure 1. AF—Anegada fault; CSC—Cayman spreading center; H—Hispaniola; HND—; LAT—Lesser Antilles trench; MAT—Middle America trench; MDF—Muertos deformed belt; NHDB—Northern Hispaniola deformed belt; NIC—Nicaragua; OF—Oriente fault; PR—Puerto Rico; PRT—Puerto Rico trench; SITF—Swan Islands transform fault; WF—Walton fault. AVES, BARB, CRO1, GUAT, ESTI, FSD0/1, JAMA, ROJO, SANA, and TEGU are site names discussed in the text.

STRAIN PARTITIONING OF THE NORTHWESTERN CARIBBEAN PLATE

GPS-determined motion of the Caribbean plate relative to North America predicts significant along-strike variations in the style of deformation along the 3100-km-long plate boundary (DeMets et al., 2000) (Fig. 1). The plate boundary extends from the Motagua Valley of Guatemala to the Lesser Antilles arc and has a GPS-derived rate of mainly left-lateral displacement of 21 mm/yr. DeMets et al. (2000) note that GPS-based interplate velocities are consistent with the along-strike transition in structural styles from (1) transtension in northwestern Central America and the western Cayman trough where divergence between the Caribbean plate vector and the trend of the plate boundary faults predicts oblique opening over a wide area; (2) pure strike-slip faulting in the central Cayman trough where the Caribbean plate vector and the trend of the plate boundary faults are parallel with strike-slip faults (Rosencrantz and Mann, 1991); (3) transpression and oblique underthrusting in the eastern Cayman trough and southern Cuba where there is convergence between plate vector and plate bounding fault (Calais and Mercier de Lépinay, 1993); (4) even greater amounts of transpression in the Hispaniola region, particularly in the zone of contact between the Caribbean plate and Bahamas Platform (Mann et al., 2002); and (5) oblique subduction of oceanic crust beneath the northeastern edge of the Caribbean plate in Puerto Rico and the Virgin Islands (Jansma et al., 2000). DeMets et al. (2000) propose a correlation between the direction of plate motion and the degree of transtension with a divergence angle between fault and plate vector of ~5° marking the threshold between predominantly strike-slip structures and predominately transtensional structures.

REGIONAL GEOLOGY AND ACTIVE TECTONICS

The western transtensional region of the North America–Caribbean margin is a diffuse plate margin with three main groups of active faults: (1) linear faults mapped along the Motagua–Swan Islands strike-slip fault zone (Plafker, 1976; Rosencrantz and Mann, 1991); (2) more discontinuous, north-trending normal faults associated with rift structures of western Honduras and Guatemala; and (3) a broad, 125–150-km-wide zone of submarine faults occupying the offshore region of shelfal to abyssal depths (200–2000 m) known as the Honduran borderlands (Pinet, 1971; Case and Holcombe, 1980). The north-trending faults of western Honduras and southwestern Guatemala bound rifts at right angles to the trend of the arcuate, strike-slip Motagua fault plate boundary (Fig. 2). These north-trending normal faults have been interpreted by previous workers as intraplate deformation and block rotations about an arcuate, convex-southward left-lateral strike-slip fault system (Plafker, 1976; Burkart and Self, 1985) and as fault termination structures related to the termination of left-lateral slip of the Motagua fault zone (Langer and Bollinger, 1979; Guzman-Speziale, 2001). In the Honduran borderlands and the Nombre de Dios range of northern Honduras, normal faults bound elongate rifts and intervening basement blocks that are subparallel to the main left-lateral strike-slip plate boundary fault (Swan Islands fault zone) (Fig. 2). The westward extent of the borderland faults disappear at the longitude of the north-trending Yojoa-Sula rift basin at 88° west (Fig. 2A).

The Motagua fault offsets a staircase of Quaternary river terraces in the Motagua Valley of Guatemala that yield long-term, left-lateral slip rates of 0.45–1.88 cm/yr (Schwartz et al., 1979). There is no quantitative estimate of the cumulative lateral offset on the Motagua fault since alluvium of the Motagua Valley obscures many of the adjoining and presumably offset rock units. The Motagua fault is directly along strike of the offshore Swan Islands fault to the east and is flanked by the active, left-lateral Polochic fault zone to the north (Burkart, 1983; Burkart, 1994) and the inactive Jocotan-Chamelecon fault zone to the south (Ritchie, 1976). The Jocotan-Chamelecon fault is inferred to be inactive because its trace has become fragmented by east-west opening of more recent, north-oriented rifts (Ritchie, 1976; Plafker, 1976). Burkart (1983) documents 130 km of left-lateral displacement on drainages along the Polochic fault that occurred between 10 and 3 Ma. Burkart (1994) proposes a chronology of plate boundary faulting that started along the Jocotan fault between 20 and 10 Ma and switched to the Polochic fault at 10 Ma, with the Motagua fault active since 3 Ma. A 230-km-long, left-lateral surface rupture averaging 1.08 m of horizontal and 0.3 m of vertical displacement occurred on 4 February 1976 along the Motagua fault of Guatemala (Plafker, 1976; Kanamori and Stewart, 1978). This M7.5 event also splayed to the south and activated ruptures along north-south oriented rift faults in Guatemala, where focal mechanisms indicated dominantly normal displacements (Langer and Bollinger, 1979).

The Swan Islands fault zone forms a prominent semi-continuous fault scarp on the seafloor (Rosencrantz and Mann, 1991). Its location is consistent with the high level of earthquake activity shown by the left-lateral earthquake focal mechanisms in the area (Fig. 2A). The fault juxtaposes oceanic crust of the Cayman trough generated at the Mid-Cayman spreading center over the past 49 m.y. with continental crust of the Honduran borderlands to the south (Fig. 2B). The Swan Islands fault steps right at the Swan Islands restraining bend, a major right-step in the left-lateral fault trace associated with topographic uplift of the Swan Islands of Honduras and active convergent deformation of the seafloor observed on sidescan and seismic reflection profiles (Mann et al., 1991). Mann et al. (1991) and Leroy et al. (2000) propose that the right step and restraining bend in the Swan Islands fault zone formed when the Mid-Cayman spreading center lengthened in a southward direction by 25 km between 19.5 and 25.9 Ma (Fig. 2B). The Swan Islands fault zone extends eastward, where part of the Caribbean–North America interplate motion is transformed into seafloor spreading along the 100-km-long Mid-Cayman spreading center (Leroy et al., 2000) and the other part of the interplate motion continues along strike-slip

faults extending along the southern edge of the Cayman trough to the island of Jamaica (Rosencrantz and Mann, 1991).

Earthquake epicenters with M > 4.0 from the National Earthquake Information Center (NEIC) database and focal mechanisms for earthquakes from the Harvard University catalog of Centroid Moment Tensors with 4.0 < M < 7.1 are compiled on a topographic basemap in Figure 2A. The greatest concentration of epicenters aligns in a belt parallel to the Swan Islands–Motagua fault zone, a continuous zone of subaerial and submarine active, left-lateral faulting that accommodates much of the present-day North America–Caribbean plate motion (Molnar and Sykes, 1969; Rosencrantz and Mann, 1991; Deng and Sykes, 1995). Earthquake focal mechanisms along this fault are dominantly left-lateral (Deng and Sykes, 1995; Van Dusen and Doser, 2000; Cáceres et al., 2005) (Fig. 2A). Earthquake events in offshore areas of the Honduran borderlands and Nicaragua Rise are widely scattered and infrequent, indicating low levels of activity in these more intra-plate areas and/or poor seismograph coverage (Fig. 2A).

Earthquake epicenters with focal mechanisms that are indicative of east-west extension are spatially associated with faults bounding north-trending rifts of western Honduras and Guatemala. Here, 12 rifts are characterized by steep, fault-bounded, intermontane valleys filled by late Miocene to Quaternary age sediments and lakes (Manton, 1987; Gordon and Muehlberger, 1994) (Fig. 2A). Guzman-Speziale (2001) used earthquake focal mechanisms in the rift area to calculate an east-west rate of extension of 8 mm/yr across all the rifts and proposed that the rifts terminate strike-slip displacement along the Motagua-Polochic fault zone.

OBJECTIVES OF THIS INVESTIGATION

Our objectives are to document active deformation south of the plate margin and variation in structural style of rifts using compilations of previous studies, tectonic geomorphology studies of onshore areas, and marine geophysical studies of offshore areas in the Honduran borderlands. Then we relate the orientation of faulting to Caribbean–North America plate motion partitioned into along-strike components of boundary-parallel strike-slip and boundary-normal extension for the western 1000 km of the margin. Finally we examine the implication of the relation of deformation styles to plate kinematics in context of the evolution of the margins since the early Miocene. The first objective—documenting the active deformation—is presented first for the onshore areas and then for the offshore areas.

ONSHORE TECTONIC GEOMORPHOLOGY AND STRUCTURE

Morphologic Indicators of Active Tectonics

In order to relate active deformation to plate margin kinematics, we first distinguish regions that are actively deforming. Onshore, we expand on three morphologic provinces defined by Rogers et al. (2002) by including interpretation of fault scarps from previous geologic mapping and interpretation of LANDSAT imagery shown in Figure 2, defining the eastern extent of rifting and its boundaries with adjacent, more tectonically stable morphologic provinces. Previously, some workers assumed that rifting is confined to western Honduras and that eastern Honduras is part of the stable Caribbean plate (e.g., Plafker, 1976; Burkart and Self, 1985), while others (Manton, 1987; Gordon and Muehlberger, 1994; Ave Lallemant and Gordon, 1999) extend active deformation to eastern Honduras.

Morphologic Provinces of Honduras

Tectonic geomorphology and hypsometric analysis reveal four main morphologic provinces within Honduras, which are outlined in white and numbered 1–4 on Figure 3A (see Rogers et al. [2002] for description of methods). Three zones originally defined by Rogers et al., (2002) are the western rifts (zone 1), the plateau (zone 2) and the eastern province (zone 3). The plateau province is subdivided into a region of inactive rifts (zone 2a) and the undeformed core plateau (zone 2b). Based on this study, the north coast (zone 4) forms a fourth morphologic region not described by Rogers et al. (2002).

The western rifts morphological province exhibits basin and range topography (zone 1, Fig. 3A) and is underlain by pre-Jurassic basement rocks, folded Cretaceous rocks, and overlying Miocene ignimbrite deposits in the western area (Rogers et al., 2002). The variable elevation in this region reflects the extreme topographic relief related to the formation of half-grabens and elevated rift shoulders (Fig. 3B). The Central American plateau originally extended across the area of zone 1, but the plateau area has been disrupted by the formation of north-trending rifts. The longitudinal profiles of the five largest rivers in the western rifts have low gradient reaches on rift valley floors but abruptly steepen when they cross onto the uplifted rift shoulders (Fig. 3C).

To the east of the active rifting, geologic mapping reveals inactive rifts formed by north-striking normal faults cutting across a terrain of pre-Jurassic basement rocks, folded Cretaceous sedimentary rocks, and Miocene volcanic deposits (King, 1972, 1973; Markey, 1995; Rogers and O'Conner, 1993) (zone 2a, Fig. 3A). Cumulative hypsometry from this area shows a hypsometric pattern similar to that observed in zone 2b, the stable core of the Central American plateau. Rivers in this zone have dominantly straight longitudinal profiles along their entire lengths river (Fig. 3C). This pattern is similar to river profiles from the plateau zone.

The plateau province (zone 2b, Fig. 3A) represents the core of the moderately dissected Central American plateau defined by Rogers et al. (2002). The rocks underlying this morphologic zone consist of pre-Jurassic metamorphic basement rocks and folded Cretaceous rocks (Rogers et al., Chapter 5, this volume). High-level erosion surfaces characterize the relatively smooth upper surface of the plateau (Helbig, 1959; Manton, 1987). Cumulative hypsometry reveals that 50% of this zone is

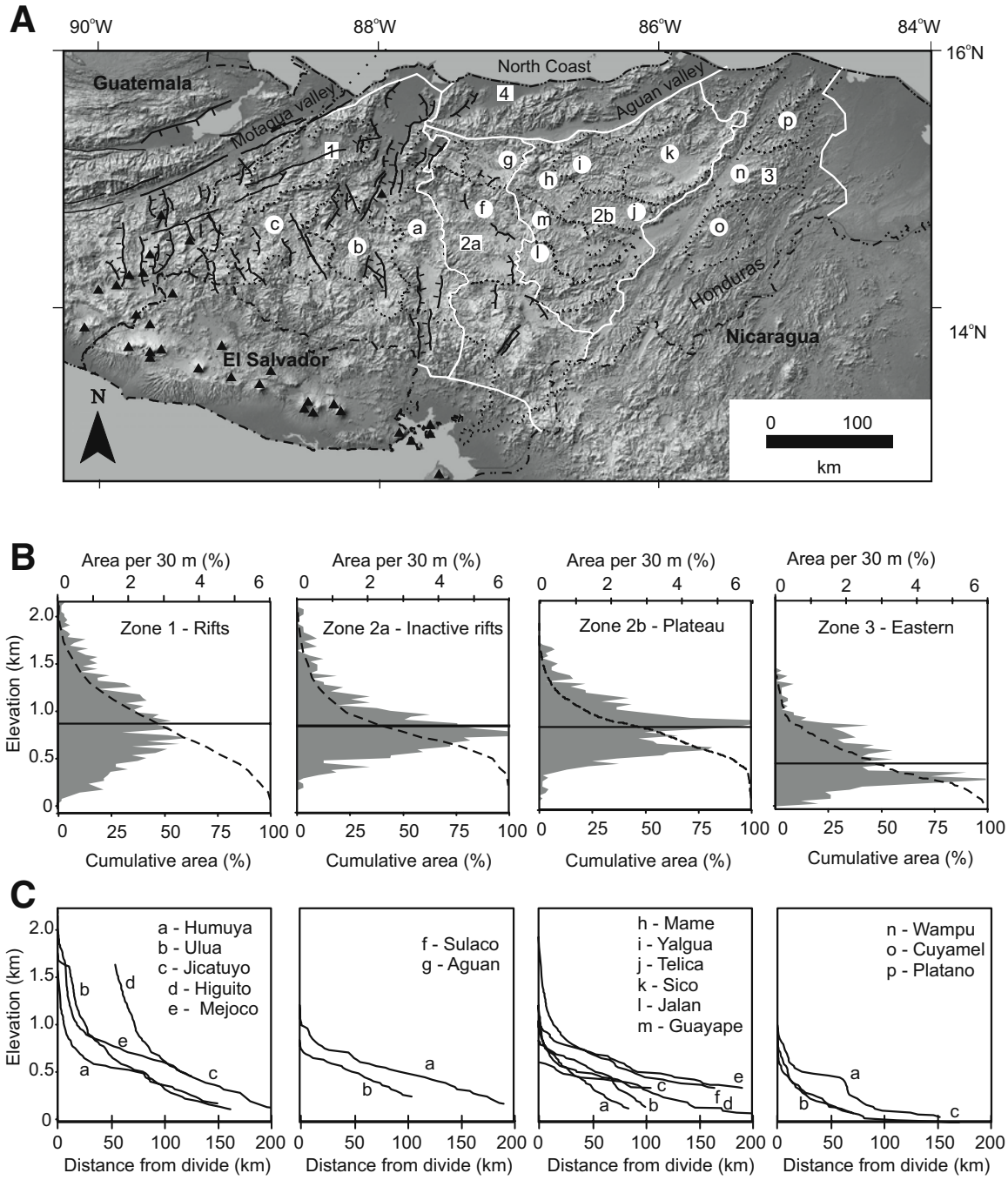

Figure 3. (A) Digital elevation model of northern Central America showing four regions of Honduras (H) outlined by white lines: Zone 1—active, north-trending rifts in western Honduras; Zone 2a—inactive rifts in central Honduras; Zone 2b—Honduran plateau; Zone 3—eastern mountains of Honduras; Zone 4—North Coast Province. Normal faults scarps from Figure 2 are shown. Watershed boundaries are shown by dotted, black lines. Solid triangles are Quaternary volcanoes. Letters defined in C. (B) Hypsometry (histogram of elevation versus area) of zones 1 through 3 in Honduras. Differential (shaded) and cumulative (dashed line) hypsometries have same vertical (elevation) axis but different horizontal axes. Solid line shows mean elevation. (C) Longitudinal profiles of trunk rivers for watersheds noted by letters in 3A. Rios Higuito and Mejoco are tributaries to Rio Jicatuyo in zone 1.

concentrated between 700 and 1000 m above sea level (masl) (Fig. 3B). The plateau is preserved because (1) it is located in an inland area removed from the Caribbean Sea and Pacific Ocean and subjected to lower rainfall amounts (1–1.5 m/yr) than surrounding areas to the west (>2 m/yr) and east (>3 m/yr); and (2) it is a tectonically stable area located on the Caribbean plate and therefore not subjected to active faulting. Six rivers in this zone have straight longitudinal profiles along their entire lengths (Fig. 3C) similar to those in the inactive rift zone. These rivers entrenched into bedrock following the uplift of the Central American plateau.

The basement rocks underlying the Eastern Lowlands of Honduras consist of pre-Mesozoic metamorphic basement rocks and folded Cretaceous rocks (Fig. 3A, zone 3) (Rogers et al., Chapter 6, this volume). This zone represents the deeply dissected eastern edge of the Central American plateau defined by Rogers et al. (2002). The longitudinal profiles of rivers in this zone display the classic concave profile of graded rivers in tectonically stable regions, adjusted to this higher rainfall area adjacent to the Caribbean Sea. The stepped profile of the Rio Wampu (Fig. 3C, profile a) is interpreted as a special case related to the breaching of its divide (the stepped area) and piracy of tributaries west of the divide.

The North Coast's Sierra Nombre de Dios and adjacent Aguan Valley (zone 4, Fig. 3A) is one of the most seismically active (Fig. 2A) and highest relief (maximum elevation: 2643 masl) areas of Honduras. In addition to these suggestions of tectonic activity, LANDSAT imagery displays the late Quaternary strike-slip and normal faulting crosscutting the region (Manton, 1987; Manton and Manton, 1999; Ave Lallemant and Gordon, 1999). In this region, deformation trends are subparallel to the plate bounding Swan Island transform and perpendicular to the north-trending rifts of the Western province (Fig. 2).

Tectonic Geomorphology of Western Rifts

Structural features aligned perpendicular to the plate margin include the north-trending normal faults and associated rifts of western Honduras and southeastern Guatemala (Plafker, 1976; Mann and Burke, 1984; Manton, 1987; Gordon and Muehlberger, 1994; Guzman-Speziale, 2001). The rifts maintain a trend almost perpendicular to the arcuate Motagua fault zone and extend from the Guatemala City graben in the west to western Honduras (Fig. 2A). These rifts are generally half-grabens, most with active eastern bounding faults. Two rifts occur in the 30-km-wide zone bounded by the Motagua and Jocotan faults and three rifts occur in the triangular wedge defined by the Middle America volcanic arc to the west and the Jocotan fault and its western extension to the north (Plafker, 1976).

Further east, the rifts assume a more northerly orientation and are wider, with larger Quaternary-filled floors. The discontinuous full grabens in this area comprise the "Honduras depression" described by Muehlberger (1976). Quaternary basaltic volcanism occurs in the rift near Lake Yojoa (Wadge and Wooden, 1982). Volcanic flows from recent cores north of Lake Yojoa have been dated using K-Ar as 0.5 Ma (ENEE, 1987).

No rifts have been studied in detail and are mainly known through 1:50,000-scale quadrangle mapping (Kozuch, 1991) incorporated into maps shown in Figures 2 and 3A. Geologic mapping reveals no evidence for Quaternary motion along the faults bounding the easternmost rifts (King, 1972, 1973; Markey, 1995; Rogers, 1995) (Fig. 2B). Gordon (1994) carried out fault striation studies on older, Tertiary rocks in western Honduras and found a complex set of extension axes that are likely related to the pre–10.5 Ma opening history of the rifts.

Because all active rifts are sharply defined topographically and appear to be currently subsiding, older, pre-Quaternary rocks characterizing their development are not exposed. Vertical motion on the faults bounding the rifts is as much as 2 km (Everett, 1970), and rifting appears to have been incipient during the deposition of middle Miocene ignimbrites (Dupré, 1970). Gordon and Muehlberger (1994) conclude that the rifting in Honduras began after 10.5 Ma, which is consistent with Hemphillian-age (9.0–6.7 Ma) mammalian fauna in the rift valley-fill deposits (Webb and Perrigo, 1984).

Tectonic Geomorphology of the North Coast

The Nombre de Dios range forms a heavily faulted dome with its core underlain by sheared high-grade gneiss and schist, felsic intrusions, and locally mafic volcanic strata of pre-Cenozoic age (Fig. 4B). Manton (1987) observes that the dominant east-northeast trend of recent faults is parallel to the trend of faults and folds in the older rocks. For a domal uplift of this large size and high elevation, younger, flanking ridges of sedimentary rocks are limited. This suggests that most of the clastic, erosional products of the uplift have been transported directly offshore into basins of the Honduran borderlands (see the section Geologic and Bathymetric Setting of the Honduran Borderlines).

The LANDSAT image in Figure 4A and the geologic map in Figure 4B display the five major faults of the Nombre de Dios range that form prominent topographic lineaments and are discussed in this section (Table 1). All faults are linear, have east-northeast strikes, and are parallel to offshore faults known from marine geophysical mapping of the offshore Honduran borderlands and Swan Islands fault zone and compiled on the map in Figure 4B.

Highly deformed marine turbidites of Miocene age are overlain by a south-dipping valley-fill conglomerate south of the city of Trujillo, indicating that the Nombre de Dios range and adjacent Aguan valley to the south may have once formed part of the submarine Honduran borderland province in pre-Miocene time (Manton and Manton, 1999). A low relief area apparent on topographic maps and imagery on the footwall of the La Esperanza fault appears to be a marine terrace and is cut by lineaments at the eastern end of the Aguan Valley, suggesting recent subaerial emergence of the terrace and continued activity of the La Esperanza fault (Fig. 4).

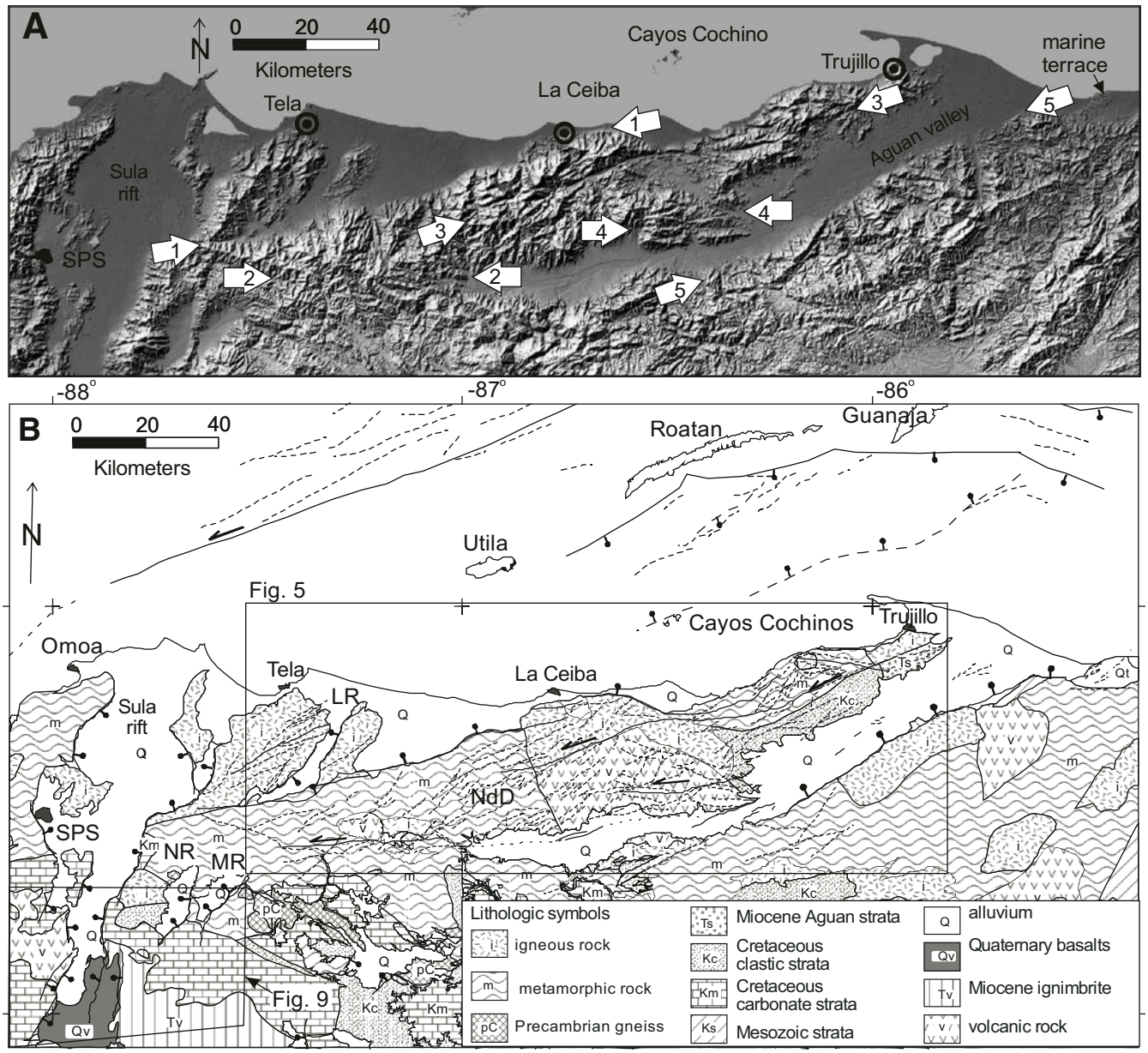

Figure 4. (A) LANDSAT image showing topographic lineaments of major faults of northern Honduras (numbered arrows are at endpoints of the following fault lineaments): 1—La Ceiba fault; 2—Aguan fault; 3—Río Viejo fault; 4—Lepaca fault; and 5—La Esperanza fault. (B) Mapped geology (Kozuch, 1991; Manton and Manton, 1999) and faults for approximately the same region as the LANDSAT image. Mapped faults are solid lines; lineaments are indicated by dashed lines. Offshore faults are taken from marine geophysical data compiled in Figure 2. Barbs indicate faults with vertical throw that form major topographic mountain fronts. Note parallelism between offshore and onshore fault trends. LR—Leon rift; MR—Morazon rift; NdD—Nombre de Dios range; NR—Negrito rift; O—Omoa; SPS—San Pedro Sula.

The Nombre de Dios range is a highly asymmetric uplift, with its drainage divide south of range midline (Fig. 5A). This asymmetry appears to be related to greater precipitation on the Caribbean side and a rainshadow on the landward (Aguan Valley) side. The north-flowing Río Cangrajal and Río Papaloteca have penetrated farthest into the Nombre de Dios range and have captured tributaries draining the south flank. This southward penetration is evidenced by remnants of a stranded paleo-divide north of and parallel with the modern divide. The modern divide is characterized by a low-relief surface interpreted as a high-elevation erosion surface. Similar, more extensive and possibly correlative erosion surfaces have been described in central Honduras south of the Nombre de Dios range and Aguan Valley (Helbig, 1959; Manton, 1987; Rogers et al., 2002) (morphologic zones 2 and 3 in Fig. 3A).

TABLE 1. NAMED FAULTS OF THE CORDILLERA NOMBE DE DIOS, HONDURAS

Fault	Number on figure	Sense of motion	Observation	Original reference
La Ceiba	1	Left-normal	Forms front of Nombre de Dios range; western terminate at edge of Sula Rift; aligns with Jocoton-Chamelcon faults to west; offsets Rio Lis Lis valley	Muehlberger (1976)
Aguan	2	Left?	Boundary between metamorphic and sedimentary rock; contiguous with linear in alluvium of western Aguan valley	Elvir (1976)
Rio Viejo	3	Left	Position along axis of range bounding high topography to north; offsets Rio Papaloteca valley	Manton (1987)
Lepaca	4	Left	Offsets Rio Lepaca and Rio Pimienta valleys	This study
La Esperanza	5	Normal-left	Southern edge of Aguan Valley	Manton (1987)

Fluvial Response to Deformation on the North Coast

To assess the activity of the five major faults (Table 1), along with previously unrecognized lineaments identified on LANDSAT imagery, we use the longitudinal profiles of rivers and streams compiled from 1:50,000 scale topographic maps with 20 m contour intervals. The east-northeast faults and lineaments of the Nombre de Dios range intersect the north- and south-flowing rivers at high angles, providing an ideal geometry for examining the effects of recent tectonic activity on the rivers (Fig. 5B). In order to test whether these lineaments represent active faults or whether they are inactive faults or some other form of layering (e.g., foliations, bedding planes, sills and dikes in basement units, joints), we compiled twelve longitudinal and representative river and stream profiles across the range from the modern drainage divide to the mountain front (Fig. 6).

North-flowing streams have convex reaches in the longitudinal profiles indicative of tectonic uplift in the Nombre de Dios range that is outpacing the rate of fluvial downcutting (cf. Hovius, 2000) (Fig. 6). Also plotted on the profiles are the derived gradient for each segment of the river calculated by taking the first derivative of the profile curve:

$$s = -dH/dL, \quad (1)$$

where s is slope, H is height, and L is distance (Hack, 1957). Parts of the stream with local areas of steep gradient are shown as the spikes or knickpoints. All knickpoints are plotted on the tectonic map of the Nombre de Dios range in Figure 5B in order to compare the locations of the knickpoints with major, mapped faults and with lineaments interpreted from the LANDSAT imagery.

The alignment on many of the profiles of lineaments and knickpoints suggests that these lineaments may be active faults that are uplifting the stream channel. Moreover, fault lineaments commonly occur downstream from convex reaches, indicating sections of the river undergoing active uplift (cf. Fig. 6, profiles 3, 5, 6, 7, 8, 9, 10, and 11). This suggests that a range-bounding fault in the knickpoint area is contributing to the upstream uplift of the upthrown block of the range. The coincidence of knickpoints, reaches of convex river profiles, lineaments, and known faults makes it unlikely that the knickpoints are solely the result of resistant lithologies in the river channels. Moreover, as annual rainfall in the Nombre de Dios range exceeds 3 m/yr it is likely that the erosive power of the rivers and streams exceeds rock resistance.

The parallel trend of the lineaments with known, active faults, like the range-bounding La Ceiba and Rio Viejo fault zones, suggests that the Nombre de Dios range is being pervasively and internally sheared (Fig. 5B). The pervasiveness of the shearing may reflect the fact that the trend of active faults is roughly parallel to the foliations and strike of older basement structures (Manton and Manton, 1999).

We identify lateral offsets of river channels in order to constrain the horizontal slip in areas exhibiting vertical uplift. Four examples of left-lateral offsets ranging from 1.5 to 2.4 km are shown on Figure 7. Bedrock-confined channels of the Río Papaloteca and Río Lis Lis are deflected left-laterally where the rivers cross the Río Viejo fault (2.4 km, Fig. 7A) and the La Ceiba fault (1.5 km, Fig. 7B), respectively, along the steep, northern mountain front of the Nombre de Dios range. The bedrock-confined channels of the Río Lepaca and Río Pimineta are deflected left by 1.7 km and 2.1 km, respectively, where they cross the Lepaca fault along the southern mountain front of the range (Figs. 7C and 7D). These data suggest that pervasive left-lateral shearing is active and accompanies the active vertical uplift constrained by the river profiles shown in Figure 6.

Meandering alluvial rivers respond to tilting perpendicular to the channel by migrating in the direction of tilt (Leeder and Alexander, 1987). The Río Aguan has migrated south, toward the La Esperanza fault, in the eastern part of its valley, indicating that the fault is mainly downthrown to the northeast and is active (Fig. 8). In the central part of the Aguan valley, the Río Aguan flows against the northern fault-bounded valley wall just south of the Lepaca uplift, indicating that the fault bounding the northern edge of the valley is downthrown to the south.

We constrain the active tilting of multiple fault blocks in the Nombre de Dios range by quantifying drainage basin asymmetry to determine the direction that a drainage basin has been tilted (Gardner et al., 1987). Drainage basin asymmetry is calculated as an asymmetry factor (AF) by the equation:

$$AF = 100(Ar/At), \quad (2)$$

where Ar is the drainage area on the downstream right-side of the trunk stream and At is the total drainage area. Drainage basin

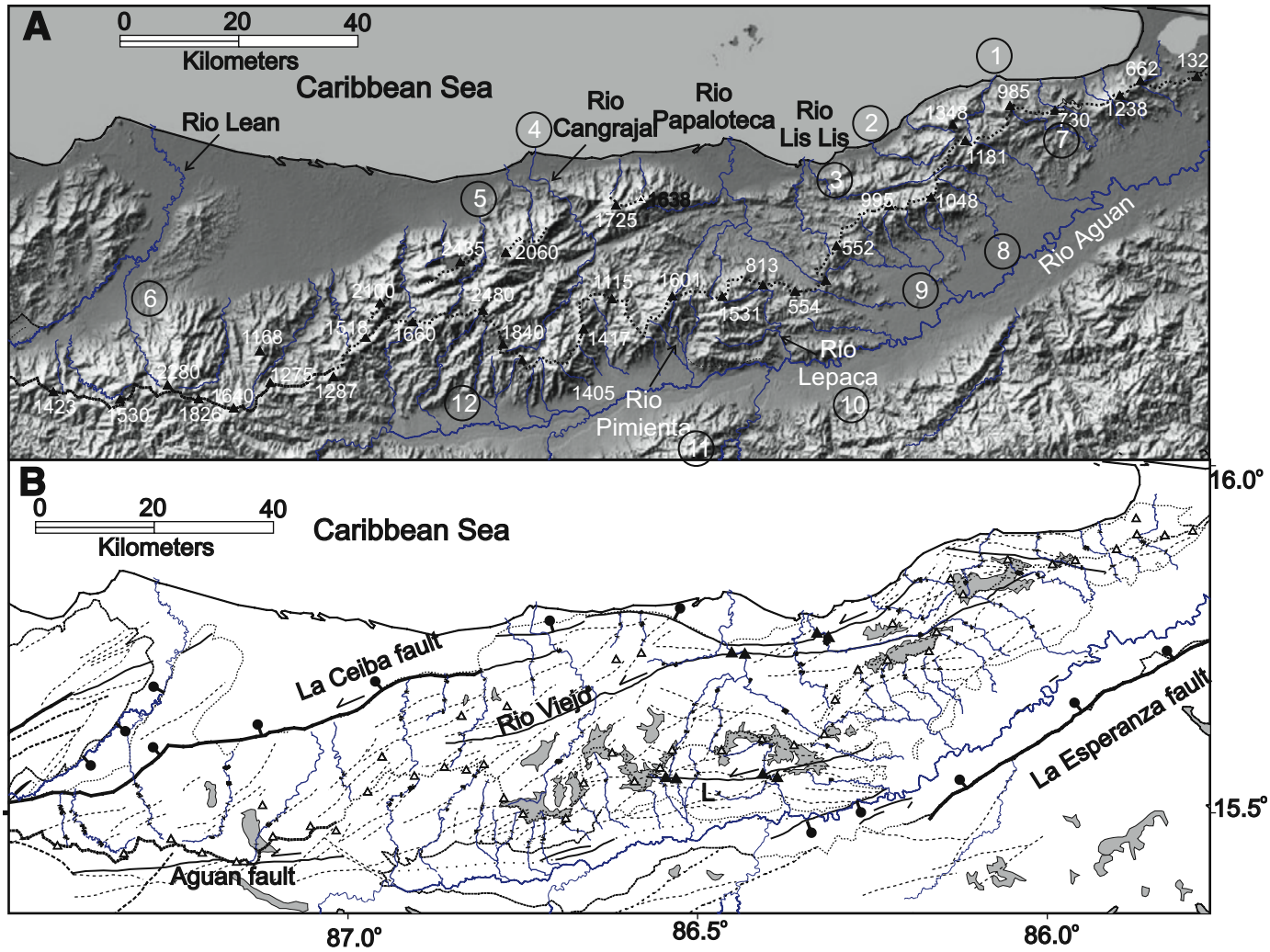

Figure 5. (A) Geomorphic features of east-northeast trending Nombre de Dios range and Aguan Valley of northern Honduras (cf. Fig. 3 for location of map area). Drainage divides are shown by heavier dotted lines. Culminations along drainage divides are shown by triangles with numbers indicated their height in meters above sea level. Note that rivers draining northward into the Caribbean are significantly longer than rivers draining southward into the Aguan Valley. Circled numbers are keyed to 12 stream profiles show in Figure 6. (B) Major lineaments and mapped faults (heavy black line, ticks on downthrown side of fault) and all lineaments interpreted from LANDSAT imagery. Steep, topographic mountain fronts along Caribbean coast and in the Aguan Valley are shown as light, dotted lines. Gray areas show low-relief surfaces preserved along the drainage divide of the ranges that are interpreted high-level erosional surfaces. Gray areas north of the modern divide are inferred as erosional surfaces formed on the previous paleo-divide prior to the southward shift to the modern divide. Apparent left-lateral offsets of river channels seen on imagery are indicated by heavy black triangles on the Río Papaloteca, Río Balfante, Río Pimenta, and Río Lepaca. Knickpoints, or localized areas of steeper river gradients from Figure 6, are shown as small black dots along rivers. L—Lepaca fault.

asymmetry for 21 north-draining watersheds and 23 south-draining watersheds of the Sierra Nombre de Dios are displayed in Figure 8.

North-draining watersheds of the western Nombre de Dios range are tilted westward, while in the central section of the range, watersheds are tilted to eastward (Fig. 8). The watersheds of the eastern part of the range near Trujillo, draining to the Caribbean Sea, are tilted westward with the exception of the easternmost watersheds. Asymmetry of watersheds draining to the Aguan valley in the western part of the range is complicated by the southward migration of the drainage divide (Fig. 5A). The central watersheds draining to the Aguan valley originate in or cross a topographic uplift centered on the Lepaca fault zone (Fig. 8). Drainage basin asymmetry reflects an eastward-plunging anticlinal uplift centered along the left-lateral Lepaca fault. Half of the eastern watersheds draining to the Aguan valley display a tilt to the west.

Topographic Development of Nombre de Dios Range

We propose several fault blocks coincident with and underlying the regions of topographic uplifts named on Figure 8:

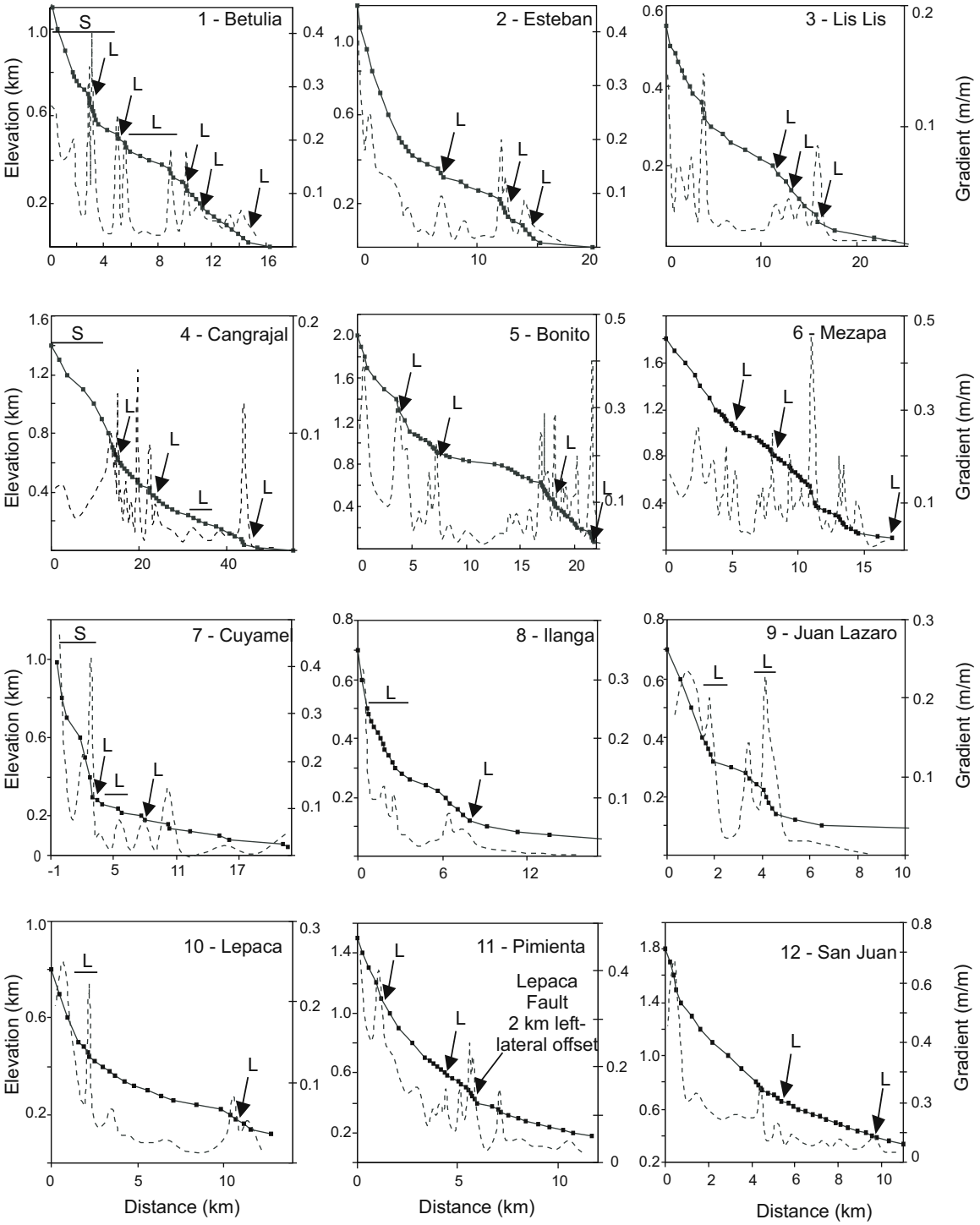

Figure 6. Stream profiles from the drainage divide to mountain fronts compiled from 1:50,000 scale topographic maps of Sierra Nombre de Dios (locations of streams, topographic divides, and topographic mountain fronts shown in Fig. 5). Solid lines show elevation of stream channels with crossings of 20 m contour interval indicated by small squares. Gradient peaks (thin line) are knickpoints. Knickpoints coinciding with mapped lineaments are labeled with "L" for "lineament" (lineaments displayed on Fig. 5B). "S" shows locations where streams cross the topographic surfaces shown in gray in Figure 5.

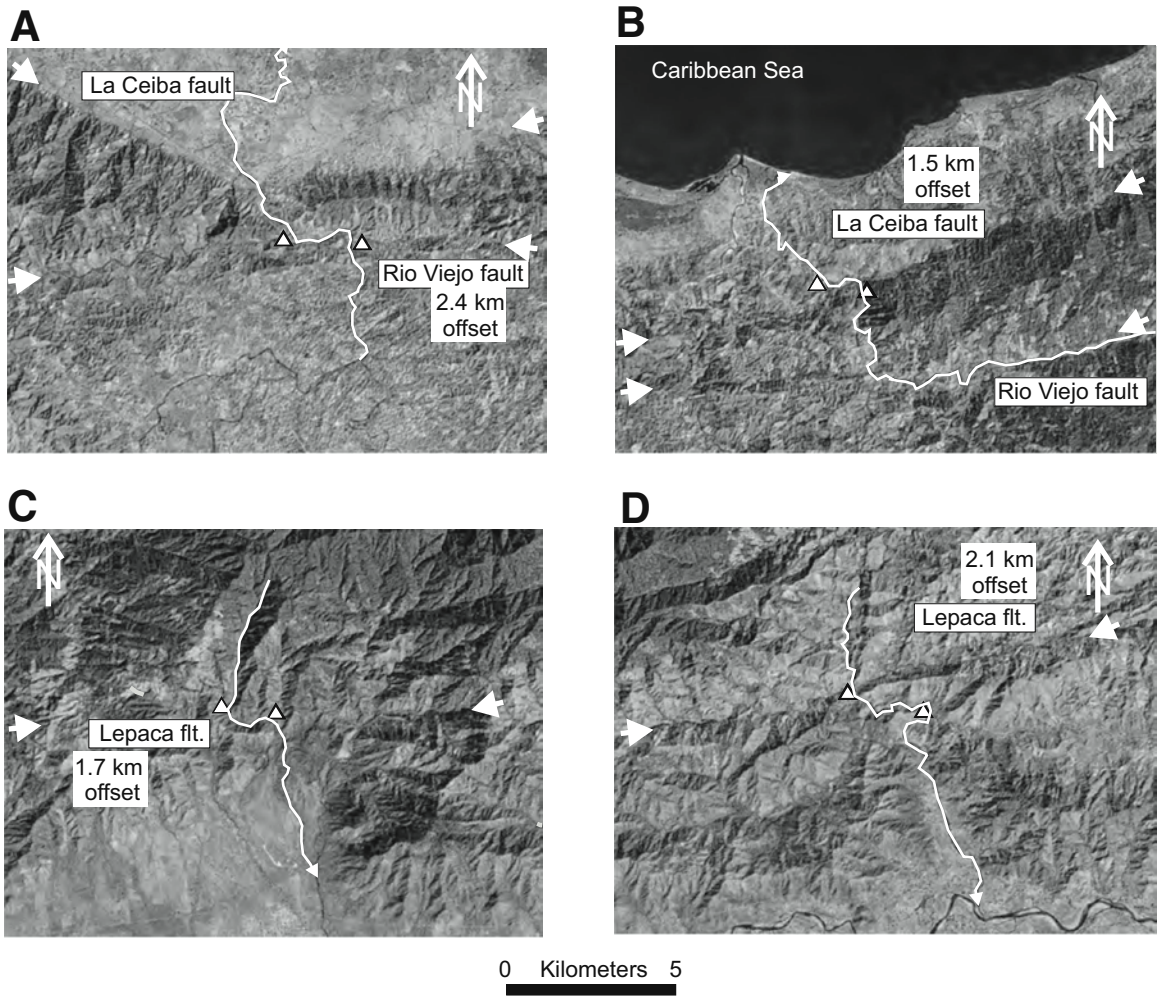

Figure 7. Four examples from LANDSAT imagery showing apparent left-lateral offsets of rivers in the Sierra Nombre de Dios (white arrows indicate fault traces shown in Fig. 5B and white triangles show magnitude of apparent left-lateral offset; locations of rivers shown in Fig. 5). All rivers shown occupy deeply incised, bedrock canyons. (A) Apparent left-lateral offset of 2.4 km of Río Papaloteca by the Rio Viejo fault. (B) Apparent left-lateral offset of 1.5 km of Río Lis Lis by the La Ceiba fault. Note that the upper reaches of this river follow the trace of the Rio Viejo fault zone. (C) Apparent left-lateral offset of 1.7 km of Río Lapaca by the Lepaca fault zone. (D) Apparent left-lateral offset of 2.1 km of southward-flowing Río Pimienta by the Lepaca fault.

1. The Pico Bonito restraining bend topographic uplift is a convergent restraining bend formed at a right-step between the La Ceiba and Rio Viejo left-lateral fault zones. Active uplift is supported by the reaches of convex river profiles shown in Figure 6, and left-lateral displacement is inferred from left-lateral river channel offsets compiled in Figures 7A–7B. Asymmetric watersheds shown in Figure 8 indicate that the bend area plunges westward.
2. La Ceiba topographic uplift is a peripheral effect related to the smaller, fault-controlled Pico Bonito restraining bend (Fig. 8). Tilt directions are variable but generally trend about a north axis.
3. Lepaca topographic uplift relates to left-lateral motion along the Lepaca fault and the formation of a large anticline parallel to the fault trace. The fault may accommodate motion along the largely buried fault along the northern edge of the Aguan Valley. Tilt directions vary across the structure.
4. Trujillo topographic uplift is related to left-lateral oblique motion along the east-northeast segment of the Rio Viejo fault zone.

Transition between the Western Rifts and the North Coast Ranges

Normal faults defining the eastern edge of the Sula rift of the Honduras depression abruptly truncate the east-northeast–striking La Ceiba fault zone (Fig. 4), and faults of the eastern boundary of the Sula rift change to more northeast trends. The

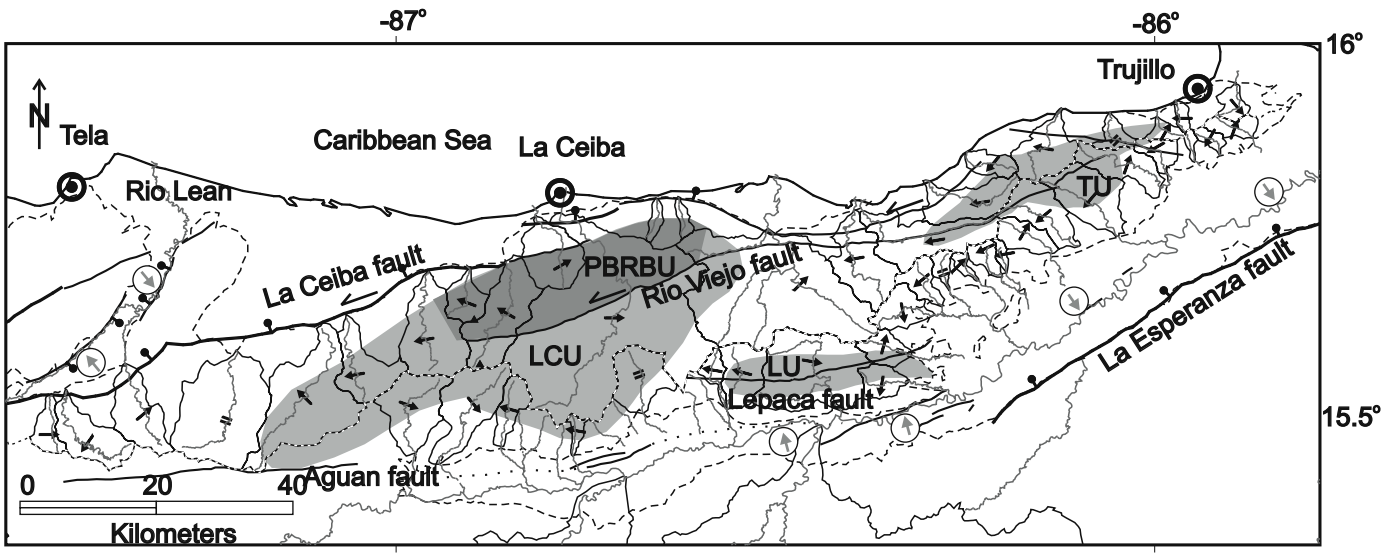

Figure 8. Comparison of topographically elevated areas associated with mapped faults of the Nombre de Dios range. The Pico Bonito restraining bend uplift (PBRBU, shown by dark shading) occurs at a right-step between the right-lateral Rio Viejo and La Ceiba fault zones. The La Ceiba topographic uplift (LCU, shown by lighter shading) borders the south flank of the PBRBU. The Lepaca topographic uplift (LU, lighter shading) is associated with the Lepaca fault zone, and the Trujillo topographic uplift (TU, lighter shading) is associated with the eastern extension of the Rio Viejo fault zone. Tectonic tilt directions are inferred from asymmetric watersheds (black arrows show direction of inferred tilting of the watershed; i.e., the larger half of the watershed is tilted toward the narrower half of the watershed). An equals sign indicates watersheds of the Sierra Nombre de Dios whose centerlines (trunk streams) are symmetrical. Arrows in open circles show tilt directions within the meandering alluvial rivers of the Aguan Valley and Lean Valley.

El Negrito and Morazon half-grabens form outliers to the east of the Sula rift but exhibit orientations more to the northeast. The RADARSAT image shown in Figure 9 documents the transition from the more northerly trends of normal faults that disrupt the Quaternary (0.5 Ma) volcanic field in the Sula rift to the more northeasterly trends of the El Negrito and Morazon rifts (average trends of rift-bounding normal faults indicated by white arrows in Fig. 9). The Lean rift is a full-graben northeast of the El Negrito and Morazon rifts and north of the La Ceiba fault (Fig. 4B). Avé Lallemant and Gordon (1999) have previously related the origin of the Lean graben to left-slip motion on the La Ceiba fault. We propose that the northeast trend of the northern Sula, El Negrito, Morazon, and Lean rifts forms a 35-km-wide rift province of intermediate orientation between the north-trending rifts of western Honduras and the east-northeast–trending rifts in the Nombre de Dios range and Aguan Valley.

OFFSHORE STRUCTURE AND STRATIGRAPHY OF THE HONDURAN BORDERLANDS

The structure and late Neogene sedimentation of the Honduran borderlands is described in papers by Kornicker and Bryant (1969) and Pinet (1971, 1972, 1975) using single-channel seismic profiling and shallow coring. We utilize deeper penetration, multi-channel seismic reflection profiles, sidescan images of the seafloor, and offshore exploration wells to better define the distribution and structure of the elongate basins and ridges underlying the Honduran borderlands. We mapped a total of 21 different basins using seismic and sidescan sonar (Fig. 2B), although more densely spaced seismic profiling may reveal that some of the basins are contiguous. The basins form a belt that narrows toward the Mid-Cayman spreading center then widens toward the west. There are two parallel basin axes, the Bonacca and Patuca, separated by an elongate basement high.

Geologic and Bathymetric Setting of the Honduran Borderlands

GEOSAT (geodetic satellite) marine gravity data compiled in Figure 10A shows the large-scale basement structure of the Honduran borderlands. To the north of the borderlands, the Cayman trough shows a large gravity low associated with thin oceanic crust produced at the Mid-Cayman spreading center between 49.3 and 0 Ma (Leroy et al., 2000). A gravity high is centered on the active spreading center of the short, 100-km-long spreading center. The Nicaragua carbonate platform, located south of the Honduran borderlands, is characterized by a smooth gravity high. The Honduran borderlands exhibits a disrupted gravity field produced by the existence of elongate, fault-bounded, margin-parallel basins and ridges characteristic of continental borderland provinces (Gorsline and Teng, 1989). Twin gravity highs or basement ridges extend along the southern, faulted margin of the Cayman trough while a gravity low basin extends along the edge of the Nicaragua Rise. A gravity or basement high, the Patuca

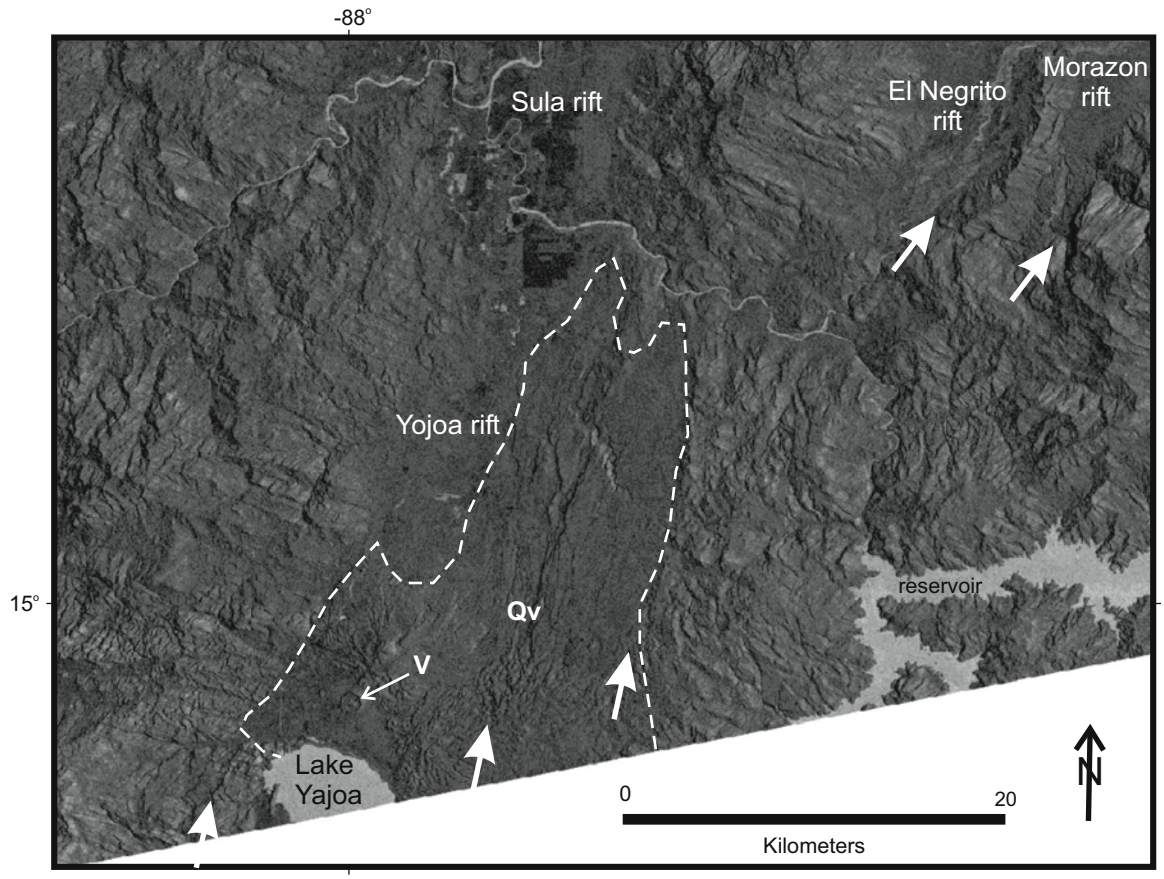

Figure 9. RADARSAT satellite image showing north-northeast–trending, late Quaternary fault scarps (white arrows) in Yojoa Quaternary basalt field (outlined by white dashed line) at the north end of Lake Yojoa within the Yojoa rift (see Fig. 4 for location of image). These scarps are mainly downthrown to the west. K-Ar age dating by ENEE (1987) shows age of field is 0.5 Ma (middle Quaternary). V—volcano; Qv—Quaternary volcanic flows.

Ridge, is present within this basinal structure and projects into the Nombre de Dios range of northern Honduras. The southern part of the Patuca Basin projects into the Aguan Valley.

The predicted bathymetry (Smith and Sandwell, 1997) of the region shown in Figure 10B is compiled along with the onshore topography. Kornicker and Bryant (1969) considered the basement and bathymetric high along the southern edge of the Cayman trough as a single ridge (Bonacca). Because regional gravity and bathymetry data show two parallel ridges, we name the features the North and South Bonacca Ridges. Kornicker and Bryant (1969) also considered the Tela Basin north of the Nombre de Dios range of northern Honduras a continuous feature extending to the northeast of Honduras, which we renamed the Patuca Basin to more accurately reflect the complex borderlands basins seen on Figure 10. The Bonacca Basin separates the North and South Bonacca Ridges and the Patuca Basin occurs between the South Bonacca Ridge and the Nicaragua Rise. The Patuca and Tela Basins are roughly collinear but are separated by a bathymetric and structural saddle northeast of Honduras. Figure 11 shows three bathymetric profiles across the Honduran borderlands correlated with the newly named basement and bathymetric features.

The twin North and South Bonacca Ridges can be identified on profiles A and B but merge on profile C (Fig. 11) to form the single, emergent Bay Islands of northern Honduras. The Swan Islands restraining bend, an active, localized restraining bend structure on the Swan Islands fault zone (Mann et al., 1991) (Fig. 2A), appears on profiles A and B but disappears along-strike on profile C (Fig. 11). The Patuca Basin forms a deep basin on profile A, which is interrupted by the appearance of the Patuca basement high on profile B. The northern half of the Patuca Basin continues westward into the Tela Basin, while the Patuca high projects into the Nombre de Dios range and the southern half of the Patuca Basin projects into the Aguan Valley. The overall effect of the parallel ridges and valleys of the Honduran borderlands is widening from east to west (Fig. 11).

Evidence of Active Tectonics and Structure

We use previously unpublished multichannel seismic (MCS) profiles across the Honduran borderlands collected during the University of Texas Institute for Geophysics (UTIG) Caribbean Tectonics (CT1) survey in 1979 combined with SeaMARC II

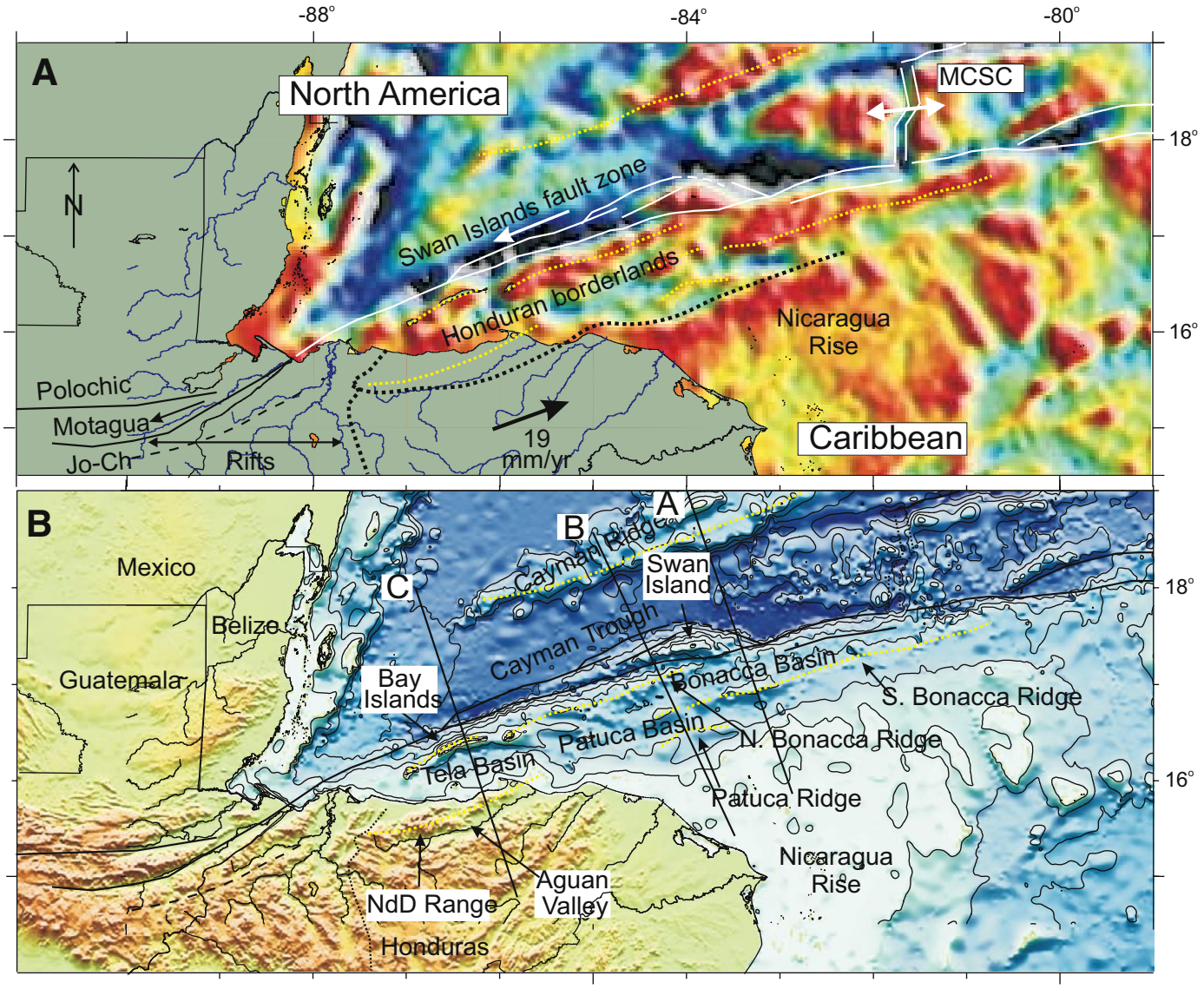

Figure 10. (A) Free-air marine gravity map of offshore areas of Honduras, Guatemala, and Belize in the Cayman trough, Mid-Cayman spreading center (MCSC), Honduran borderlands, and Nicaragua Rise (gravity data from Sandwell and Smith, 1997). Hot colors represent relatively higher gravity values above basement ridges; cooler colors show sediment-filled basins between basement ridges. Fault locations taken from fault compilation shown in Figure 2. Arrow shows Caribbean plate motion vector in Honduras relative to a fixed North American plate. Dotted lines correspond to crests of major basement ridges identified by name in Figure 10B. The northern edge of the Honduran borderlands is defined by the Swan Islands fault zone; the southern edge of the borderlands is defined by the Nicaragua Rise offshore and the Aguan Valley onshore. Jo-Ch—Jocotan-Chamelecon faults. (B) GTOPO30 digital elevation model of Central America merged with gravity-derived GTOPO5 bathymetry of offshore areas of Honduras from Smith and Sandwell (1997) (bathymetric contours are 1000 m, except for 100 m contour near shore). Yellow lines represent crests of bathymetric ridges and correspond to the yellow lines shown in the gravity map. NdD—Nombre de Dios.

sidescan sonar images and single-channel seismic lines of the seafloor and shallow subsurface collected in 1989 (Rosencrantz and Mann, 1991; Mann et al., 1991) to document and map active faults and their relation to observed bathymetry and structure. We consider faults breaking young seafloor sediments to be "active." The sidescan imagery was used in conjunction with the MCS profiles to verify that the faults extend to the seafloor and to map curving and anastomosing faults between MSC lines. The locations of the MCS and single-channel seismic (SCS) seismic lines used in the study are shown on Figure 2B; the footprint of the sidescan image is shown on Figure 2A.

MCS profiles CT1-8a and CT1-8b trend north-northwest and provide a cross section of ~4 s two-way travel time (TWTT) of the eastern part of the Honduran borderlands southeast of the

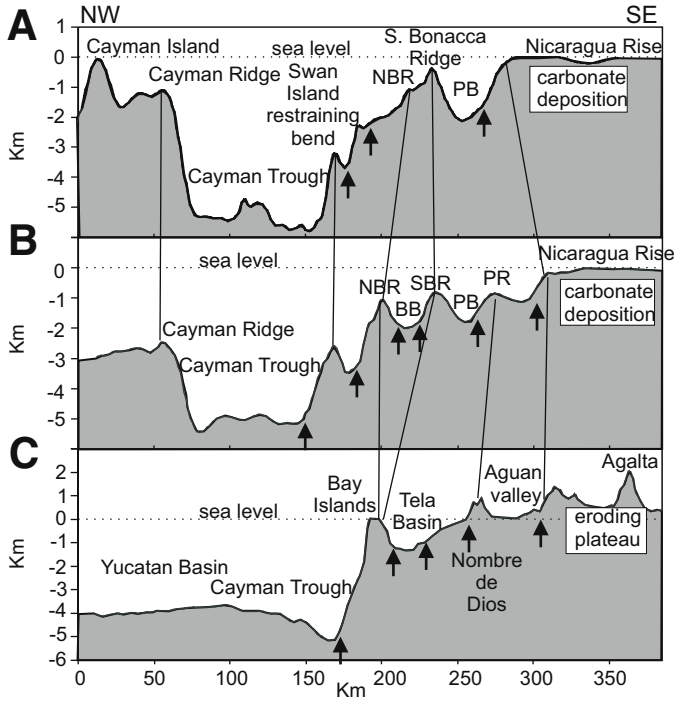

Figure 11. Bathymetric profiles A, B, and C across the Honduran borderlands and northern Honduras showing along-strike correlation of the main east-northeast–trending bathymetric ridges and flanking basins (cf. Figure 10B for locations of profiles). Arrows show positions of major active faults from Figure 2. Lines from profile to profile display features that correlate. Note the overall east to west widening of the basins consistent with the predictions for east to west increase in extension shown in Figure 18A. BB—Bonacca Basin; NBR—North Bonacca Ridge; PB—Patuca Basin; PR—Patuca Ridge; SBR—South Bonacca Ridge.

Swan Islands restraining bend (Fig. 2B). Seven active faults are recognized: two are parallel strands of the Swan Islands fault zone (see Rosencrantz and Mann, 1991), and five bound the Bonacca and Patuca Basins and separate them from the intervening basement highs, the North and South Bonacca Ridges (Fig. 12A). Correlation of line CT1-8 with the sidescan image in Figure 13B shows that a linear fault along the crest of the South Bonacca ridge forms a major scarp on the seafloor, indicating an active feature. This fault forms one edge of a large basement ridge with normal faults dipping away from its center (Fig. 13C).

MCS profile CT1-6a and CT1-6b trends north to a depth of ~5 s TWTT in the central part of the Honduran borderlands southwest of the Swan Islands restraining bend (Fig. 2B). Five active faults are recognized: three are parallel strands of the Swan Islands fault zone (highlighted by white arrows in Fig. 14B) and two bound the South Bonacca Ridge (Fig. 12A). Correlation of line CT1-6 with the sidescan image in Figure 14B shows linear fault scarps along the en echelon crest of the North Bonacca ridge. A southeast-dipping normal fault forms a half-graben (Bonacca Basin) filled with asymmetric wedge-shaped seismic unit 2 (Fig. 14C). Normal faults bounding the symmetrical Patuca graben at the south end of the seismic line also penetrate the seafloor (Fig. 14D).

MCS profile CT1-3b is the westernmost MCS line and trends northward across the borderlands (Fig. 2A). This line displays the steep scarp of the Swan Islands fault zone (indicated by the white arrows in Fig. 15B) at the edge of the Cayman trough, a series of six half-grabens formed along southward dipping normal faults, and tilting and faulting of sequence 3, suggesting that the rift process is ongoing (Fig. 12C).

Both the Bonacca and Patuca rifts are much wider on line CT1-6ab than on line CT1-8ab to the west, supporting the basic observation of the north-south widening of the Honduran borderlands from east to west seen on the regional bathymetric profiles in Figure 11.

SCS line 71, collected in 1989 along with the sidescan data, trends east to west across the Tela Basin (Fig. 16A). Line 71 images two active fault scarps seen as faint lineaments on the sidescan image (Fig. 16B). In the subsurface, these faults control small east-northeast–trending rifts within the Tela Basin (Fig. 16C).

Stratigraphic Development of the Honduran Borderlands

Three distinct seismic sequences are identified on the seismic profiles and are numbered 1, 2, and 3 on Figure 12. The lowest sequence, sequence 1, consists of tabular, tilted reflectors up to 1.0 seconds TWTT in thickness (Figs. 13C and 14C). The base of this sequence merges with the acoustic basement due to loss of energy with depth and therefore the nature of the contact between sequence 1 and basement is not clear. Seismic facies associated with sequence 1 include a semi-continuous high-amplitude facies consisting of subparallel, semi-continuous high-amplitude reflections with high-amplitude reflections dominant suggesting sand-rich channel-lobe complexes. Based on its geometry, we interpret tabular sequence 1 as a pre-rift unit deposited prior to the formation of the full and half-grabens seen on the profiles. The parallel, horizontal reflectors indicate that this unit was deposited as a flat layer above a continental or island arc crust at the northern edge of the Nicaragua Rise.

Sequence 2 consists of a wedge-shaped, isolated, fault-bounded package of reflectors indicative of long-term vertical motion on the adjacent fault scarps (Figs. 13C, 13D, 14C, 14D, and 15C). Seismic facies associated with sequence 2 include a semi-continuous high amplitude alternating with low-amplitude facies containing concave-up high-amplitude reflections and wedge-shaped external configuration, suggesting partially channelized turbidite lobe complexes. For example, on Figure 13C, the wedge-shape of sequence 2 is imaged adjacent to the presently active basement block (South Bonacca Ridge) and linear fault shown in Figure 13B. On Figure 13D crossing the Patuca Basin, sequence 2 forms two similar wedges against normal faults dipping to the southeast. We interpret wedge-shaped sequence 2

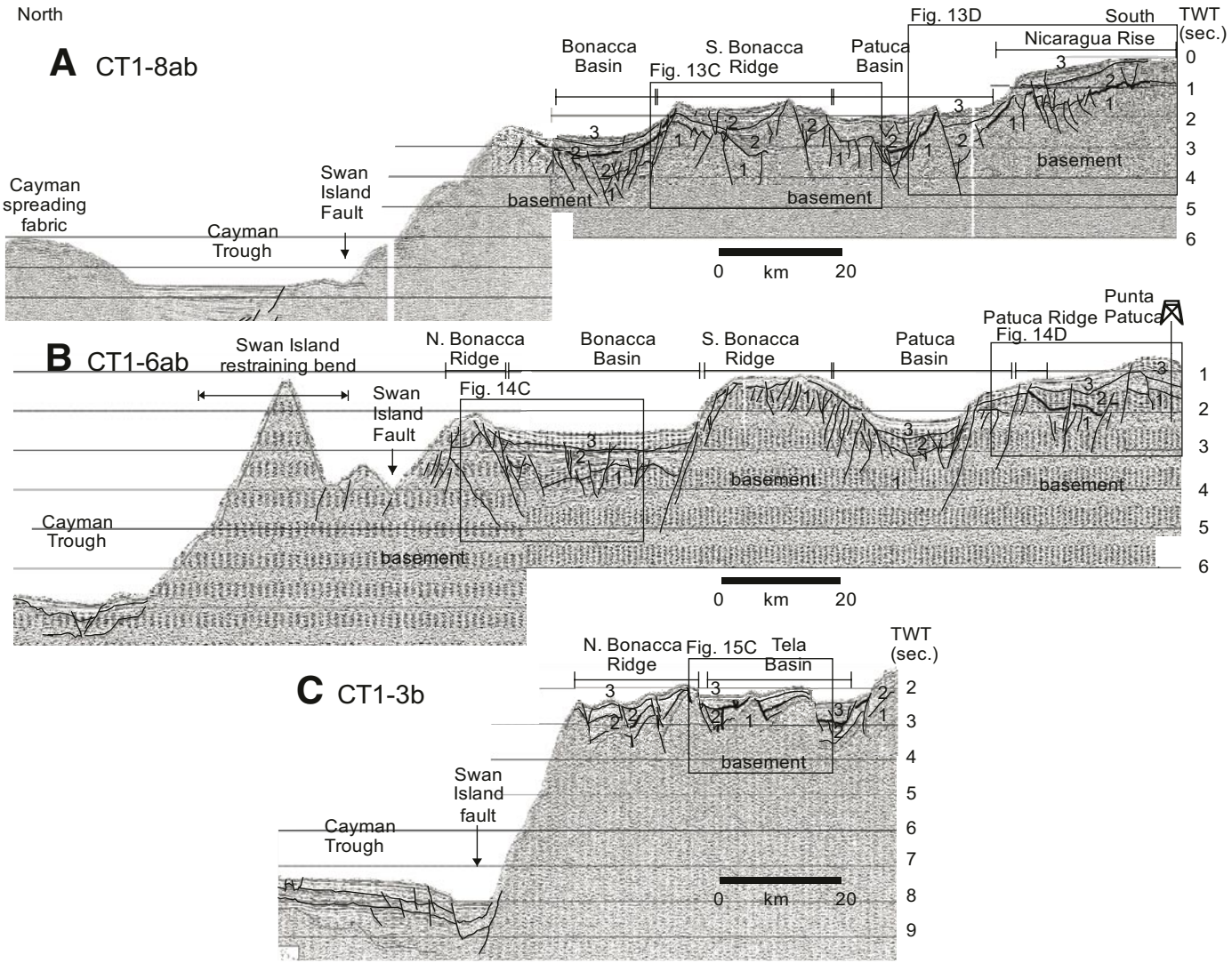

Figure 12. (A) Interpreted University of Texas Institute for Geophysics multi-channel seismic (MCS) line CT1-8ab across half-grabens and intervening basement horsts of the Honduran borderlands and the southern part of the Cayman trough. Depth is in two-way time (TWT). Three main unconformity-bound sequences are Sequence 1—a lower, pre-rift sequence; Sequence 2—a syn-rift sequence; and Sequence 3—a late syn-rift sequence. Boxes show locations of blowups shown in Figures 13C and 13D. (B) Interpreted UTIG MCS line CT1-6ab. Boxes show locations of blowups shown in Figures 14C and 14D. (C) Interpreted UTIG MCS line CT1-3b. Box shows location of blowup shown in Figure 15C. Note the top (east) to bottom (west) increase in the width of the Bonacca Basin and deepening of the Patuca Basin.

as a syn-rift unit that accompanied the main phase of rifting and fault scarp formation.

Sequence 3 is the uppermost unit and provides a tabular fill of the basinal areas of the Bonacca and Patuca Basins (Figs. 13C, 13D, 14C, and 14D). A progradational, shingled facies displays a basinward progradation geometry of reflectors that changes downdip into semi-continuous high amplitude facies. Sequence 3 is interpreted as a post-rift unit. Fault control on tabular sequence 3 is less strong than on the wedge-shaped units of sequence 2. Nevertheless, some fault scarps penetrate unit 3 to the seafloor and indicate that faulting continues today although generally not forming rifts with clastic wedge units (cf. Figs. 13C and 13D). The source of sediment for sequence 3 is either peri-platform carbonate ooze derived from carbonate production on the Nicaragua Rise (cf. Fig. 13D) or terrigenous clastic material derived from major river systems of northern and eastern Honduras (Fig. 10B).

This proposed rift interpretation is similar to that proposed by Pinet (1975) based on his study of single-channel seismic reflection study in the area of the Tela basin (Fig. 2A). Pinet (1975) documented two stratigraphic sequences above an angular unconformity disrupted by normal faults that form horsts and grabens

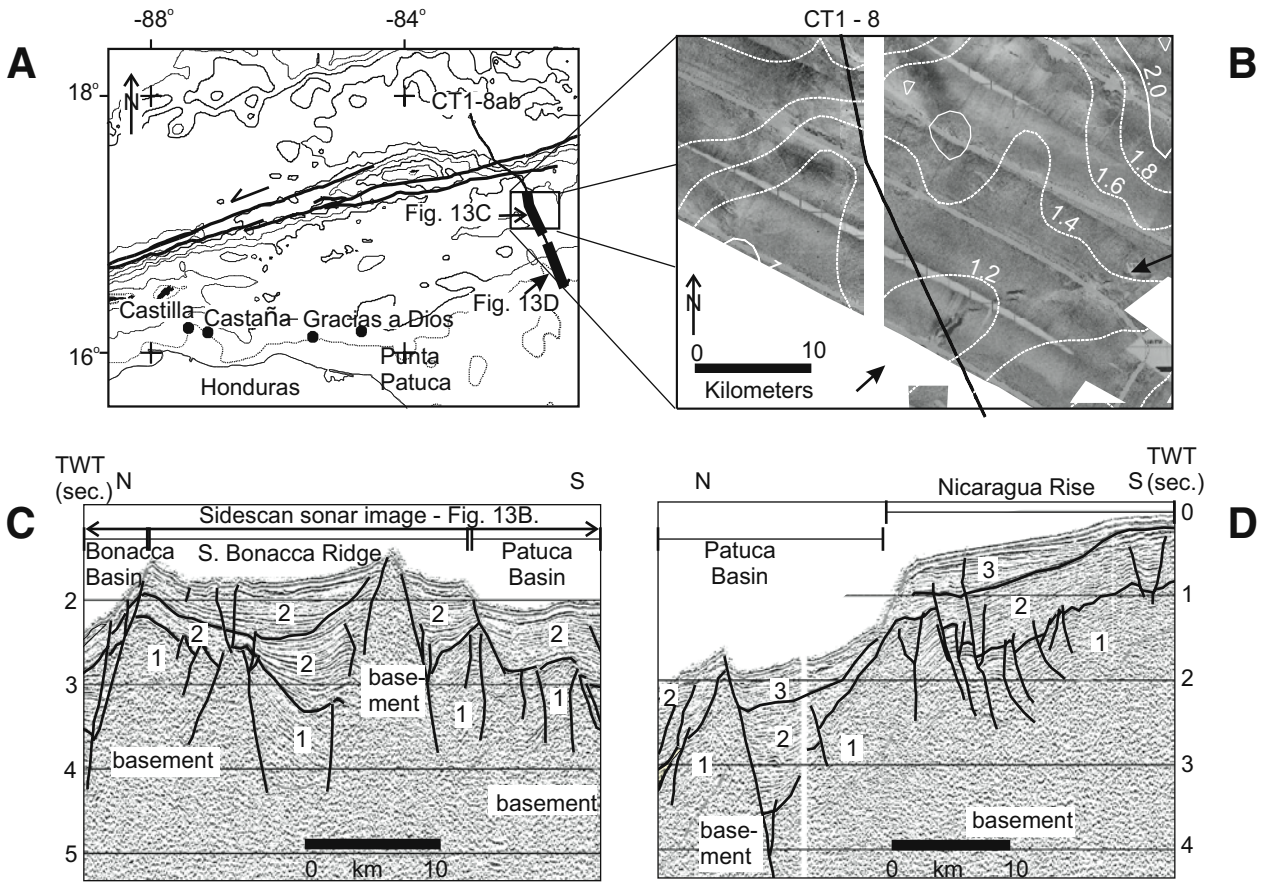

Figure 13. (A) Bathymetric map showing track of University of Texas Institute for Geophysics multi-channel seismic (MCS) line CT1-8ab relative to the Swan Islands fault zone, the Honduran coastline, and four offshore exploration wells. Bold segments of track indicate locations of seismic lines shown in C and D. Boxed area shows location of the SeaMARC II sidescan sonar image of seafloor expression of South Bonacca Ridge shown in B. (B) Sidescan image of seafloor overlying area imaged by line CT1-8ab showing crest of the South Bonacca Ridge (indicated by black arrows). Bathymetric contours are in kilometers (200 m contour). (C) Segment of MCS line CT1-8ab showing South Bonacca Ridge and flanking Bonacca Basin to the north and Patuca Basin to the south. Note fanning of syn-rift seismic sequence 2 indicative of vertical throw on the South Bonacca horst. (D) Segment of MCS line CT1-8ab showing fault scarp cutting youngest sequence 3 in the Patuca Basin. Note contrast in asymmetry between sequences 2 and 3 indicating that the recent phase of extension may be weaker than the phase responsible for sequence 2. TWT—Two-way time.

filled by turbidites (Fig. 2A). Noting that these sequences are uniform in thickness, Pinet (1975) inferred that the block faulting postdates the deposition and proposed a late Miocene–Pliocene age of deposition and a Pliocene normal faulting event based on correlation to onshore geologic history.

Four oil exploration wells (Fig. 17) drilled at shelfal to slope water depths (66–337 m below sea level [mbsl]) along the southern edge of the Honduran borderlands adjacent to the Patuca rift basin (Fig. 2B) allow correlation between the dated units in the wells and seismic units 1–3. Sonic log data from Punta Patuca-1 was converted to two-way travel time and this time section was then correlated to the south end of MSC profile CT1-6ab crossing the Patuca basin (Fig. 14D). The Punta Patuca-1 well was drilled in an area outside of the main zone of rifting in the deeper water Patuca basin. Despite this, all four wells show a similar history, suggesting that the general timing and lithologies of the wells provide a reliable insight into the rift history of the Honduran borderlands. The four wells, drilled to depths of 2397–3790 m, penetrated a basement of variable lithologies (Fig. 17). Above a basal unconformity, the overlying rock types range from Early Cretaceous through late Eocene (Fig. 17). Clastic rocks of middle Miocene age overlie the unconformity and range in water depth from subaerial (?) redbeds to coastal or coastal shelf. We interpret this contact as middle to early late Miocene transition from the acoustic basement to the overlying tabular pre-rift seismic unit 1 (Fig. 12). Syn-rift seismic unit 2

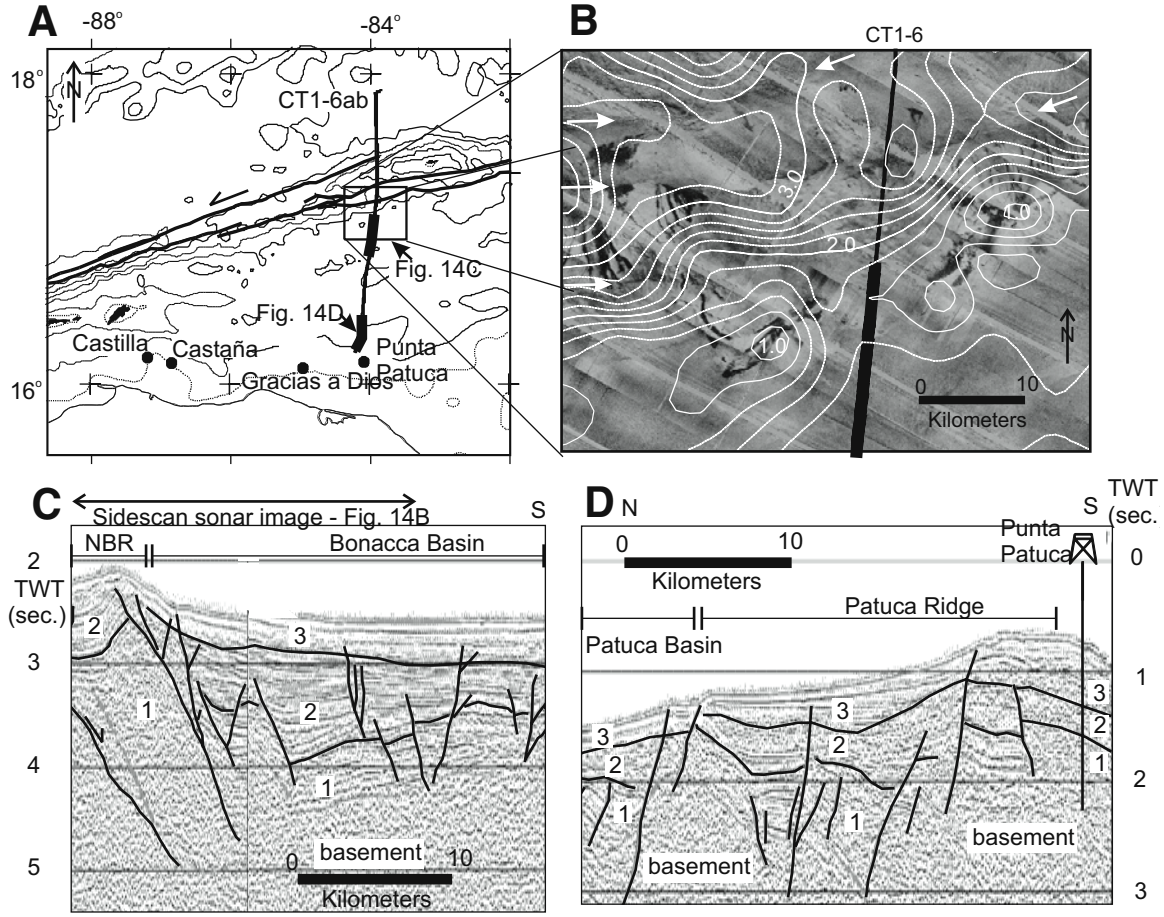

Figure 14. (A) Bathymetric map showing track of University of Texas Institute for Geophysics multi-channel seismic (MCS) line CT1-6ab. Bold segments of track indicate locations of seismic lines shown in C and D. Boxed area shows location of the SeaMARC II sidescan sonar image of seafloor expression of North Bonacca Ridge shown in B. (B) Sidescan image of seafloor overlying area imaged by line CT1-6ab showing fault strands of the active, left-lateral Swan Islands fault zone indicated by white arrows and crest of the North Bonacca Ridge. (C) Segment of MCS line CT1-6ab showing North Bonacca Ridge and flanking Bonacca Basin to the south. Note fanning of syn-rift seismic sequence 2. Emergent horst block and faults with seafloor expression indicates active faults. (D) Segment of MCS line CT1-6ab showing sequences 1–3 and position of Patuca Ridge on which the Punta Patuca well was drilled in 1978 (cf. Fig. 17; well location was projected 9 km onto this line). Note faults extending to seafloor. TWT—Two-way time.

correlates to a late Miocene section of sandstone and shale with minor shallow marine limestone in the Punta Patuca well. Post-rift seismic sequence 3 correlates to a Plio-Pleistocene section of mudstone deposited at bathyal depths.

The Castaña-1 drilled near the mouth of the Río Aguan and the bathymetric high that separates the Tela and Bonacca Basins penetrated 400 m of limestone, which is suggestive of localized clastic bypass and carbonate deposition on the bathymetric high. Numerous bentonite horizons along with volcanic fragments found in the middle Miocene clastic shelf strata of Punta Patuca-1 and Gracias A Dios-1 represent airfall and fluvial linkage to the ignimbrite province of the Miocene arc of Central America (Sigurdsson et al., 2000; Jordan et al., this volume).

ACTIVE DEFORMATION RELATED TO PLATE KINEMATICS—TWO STYLES OF TRANSTENSIONAL DEFORMATION

We have presented geologic, earthquake, marine geophysical, and remote sensing data to show that Neogene to Recent transtensional deformation produced at the North America–Caribbean plate boundary in northern Central America exhibits two distinct structural styles. East-west extension along faults normal to the plate boundary occurs south of the western 375-km-long plate boundary segment, producing basin and range morphology in western Honduras and southern Guatemala. To the east, NNW-SSE extension along faults subparallel to the

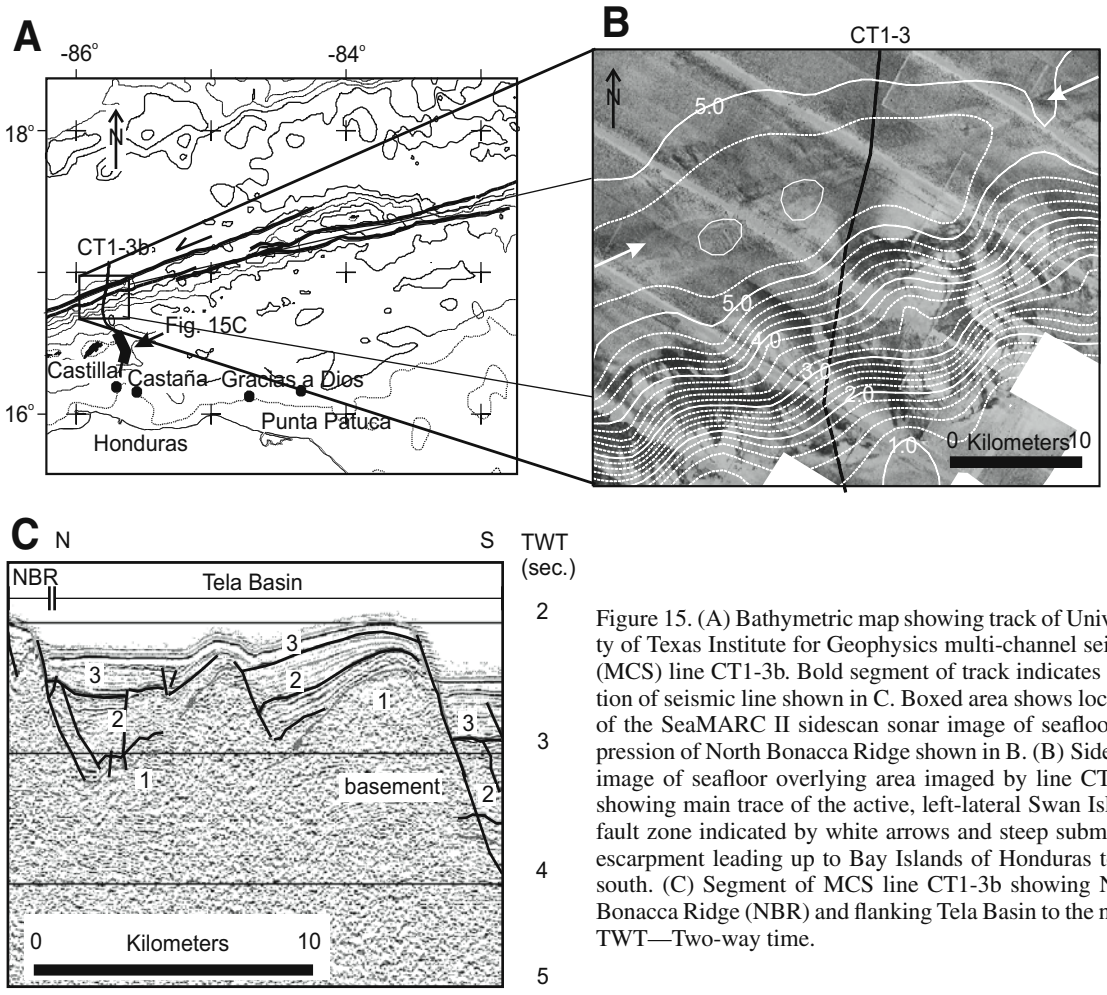

Figure 15. (A) Bathymetric map showing track of University of Texas Institute for Geophysics multi-channel seismic (MCS) line CT1-3b. Bold segment of track indicates location of seismic line shown in C. Boxed area shows location of the SeaMARC II sidescan sonar image of seafloor expression of North Bonacca Ridge shown in B. (B) Sidescan image of seafloor overlying area imaged by line CT1-3b showing main trace of the active, left-lateral Swan Islands fault zone indicated by white arrows and steep submarine escarpment leading up to Bay Islands of Honduras to the south. (C) Segment of MCS line CT1-3b showing North Bonacca Ridge (NBR) and flanking Tela Basin to the north. TWT—Two-way time.

plate boundary occurs south of a 600-km-long plate boundary segment, producing margin-parallel ridges and basins onshore in northern Honduras and in the offshore Honduran borderlands region (Fig. 18A).

In the western area, the north trending normal faults have been interpreted as (1) intraplate deformation and block rotations about a highly arcuate, convex-southward left-lateral strike-slip fault system (Plafker, 1976; Burkart and Self, 1985); and (2) fault termination structures related to the termination of left-lateral slip of the Motagua fault zone (Langer and Bollinger, 1979; Guzman-Speziale, 2001). While transtensional deformation has not been proposed previously for the Honduran borderlands and Nombre de Dios range and Aguan Valley of northern Honduras, we show that east-northeast–trending faults are oblique-slip and extend in a zone ~150 km south of the Swan Islands fault.

We compare the orientation of active faults with the trend of GPS-derived Caribbean plate motion vectors (Fig. 18). The three plate vectors shown are for points along the Motagua–Swan Islands fault system at longitudes 89°W, 85°W, and 81°W and are decomposed to show the extensional and strike-slip component of the plate vector. The extensional component of motion is controlled by the angular divergence (Fig. 18B) between the plate vector and the trend of the plate boundary fault. The extensional component of the plate vector increases from 0.2 mm/yr at longitude 81°W near the Mid-Cayman spreading center to 4.8 mm/yr at longitude 89°W in the Motagua Valley of Guatemala and is consistent with the widening of plate margin deformation from east to west.

The angular difference (Fig. 18B) remains relatively constant and <5° in the eastern area of the Mid-Cayman spreading center that is characterized by strike-slip faulting on well-defined faults (Rosencrantz and Mann, 1991). The value increases to amounts >5° in the central area adjacent to the offshore Honduran borderlands and increases up to 20° in the area of the Motagua Valley. East-west extension on faults normal to the plate margin occurs when the angle of divergence between the main plate boundary fault (Motagua fault zone) and the GPS-derived Caribbean plate vector is ≥10° (Fig. 18). NNW-SSE transtension on faults subparallel to the plate boundary occurs when the angle of divergence between the plate boundary fault and the Caribbean motion vector is between 5 and 10°. A narrow, 35-km-wide

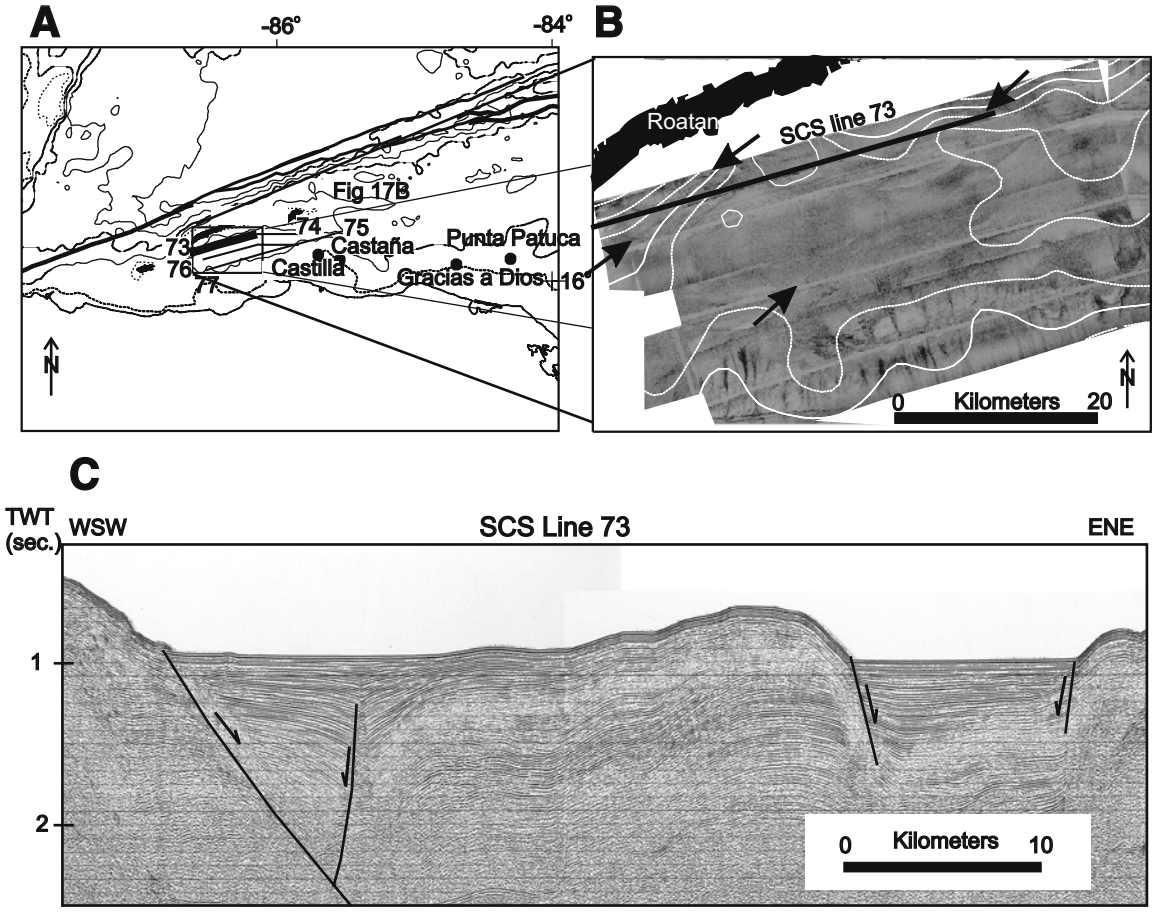

Figure 16. (A) Bathymetric map showing track of University of Texas Institute for Geophysics single-channel seismic (SCS) line 73. Bold segment of track indicates location of seismic line shown in C. Boxed area shows location of the SeaMARC II sidescan sonar image of seafloor expression of the Tela Basin adjacent to Roatan, Bay Islands, Honduras, shown in B. (B) Sidescan image of seafloor overlying area imaged by line 73 showing traces of two faults breaking the seafloor indicated by white arrows that trend east-northeastward. (C) Blowup of segment of SCS line 73 showing rift structures affecting the youngest units of the basin (Plio-Pleistocene turbidite fill penetrated in the wells on the east flank of the deep basin). Lack of penetration on SCS line 73 does not allow recognition of sequences 1, 2, and 3 as observed on UTIG multi-channel seismic lines.

tectonic transition area in north-central Honduras separates the north-trending rifts of western Honduras and from the boundary-parallel rifts in northeastern Honduras and the offshore Honduran borderlands (Fig. 18).

Estimated partitioning of the Caribbean–North America velocity components into parallel (strike-slip faulting) and perpendicular (normal faulting) to the trend of the plate boundary faults is derived by rotating the predicted plate velocities using the DeMets et al. (2000) pole information onto local fault trends at the locations separated by ~50 km (Fig. 18C). Values of strike-slip remain relatively constant around 18 mm/yr except for a decrease to 17 mm/yr in the area of maximum predicted extension near the eastern end of the Motagua Valley (Fig. 18C). Extension varies but clusters around the median 0° line in pure strike-slip areas of the Oriente fault and Mid-Cayman spreading center. To the west, extension increases to a maximum of 6 mm/yr in the Motagua Valley near longitude 88.5°W (except near the Swan Islands restraining bend near longitude 84°W).

NNW-SSE extension along faults subparallel to the plate boundary in the Honduran borderlands and northern coast of Honduras coincides with extensional partitioning rates <5 mm/yr. E-W extension on faults normal to the plate boundary in western Honduras and Guatemala coincides with extensional partitioning rates >5 mm/yr.

GEOLOGIC EVOLUTION OF THE BORDERLAND REGION

We address the Neogene evolution of transtension south of the North America–Caribbean plate boundary in two ways. First, we quantify the amount of extension that has occurred in both the offshore borderlands region and also in the western

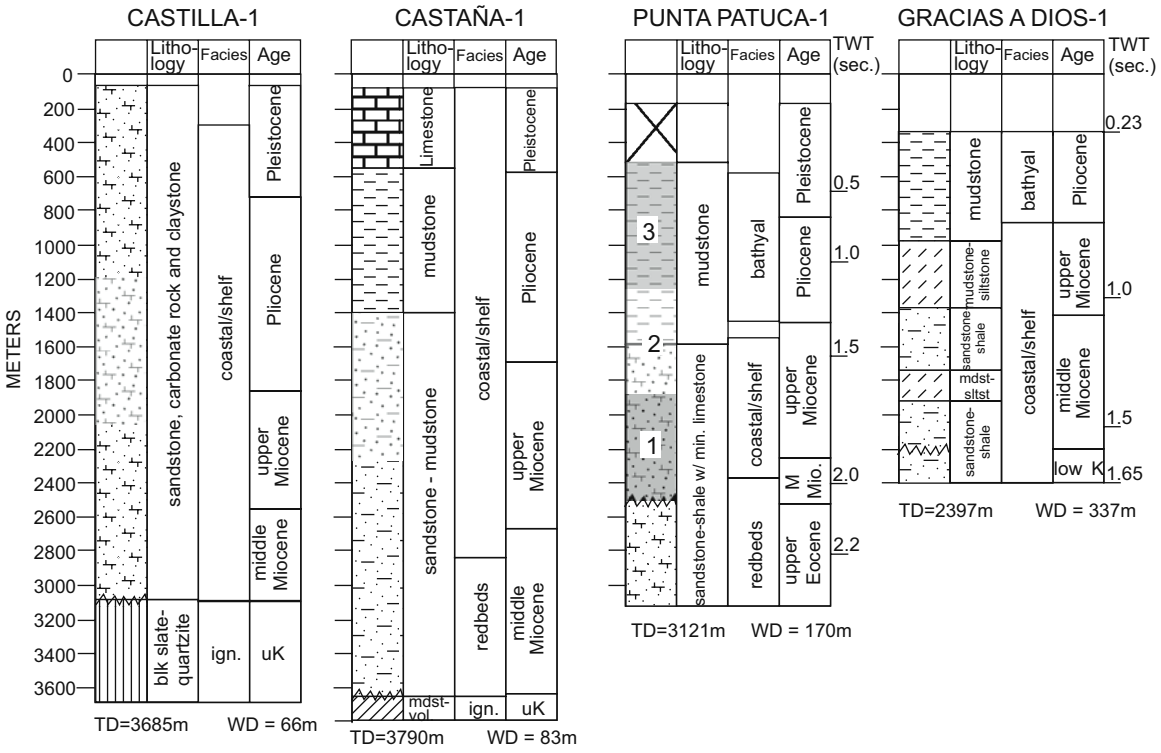

Figure 17. Well logs from four offshore exploration wells from the Honduran borderlands (well logs were provided by and used with written permission from the Dirección de Energía of Honduras). Sonic log data available for Punta Patuca-1 and Gracias a Dios-1 wells was used to convert well logs to two-way time sections that were then correlated to multi-channel seismic time sections. This correlation showed that pre-rift sequence 1 is middle to early late Miocene in age, syn-rift sequence 2 is late Miocene, and late syn-rift sequence 3 is Pliocene and younger. Note the large unconformity at the base of the middle Miocene.

rifts. Next, we utilize these results along with regional geologic and plate kinematic constraints to develop a quantified plate reconstruction of this transtensional margin as it developed during the Neogene.

Regional Extension

Individual rifts of the Honduran borderlands widen from east to west (Fig. 11). This trend can be explained by more extension in the west during the development of the rifts, as suggested by the distribution of instantaneous strain displayed in Figure 18. To estimated the finite strain during evolution of the rifts, we restore the three seismic lines (CT1-8ab, CT1-6ab, and CT1-3 from Fig. 12) using the vertical shear fault restoration method (Rowan and Kligfield, 1989). We take the top of the middle Miocene–age seismic sequence 1 (Fig. 12) as the pre-rift datum for the reconstruction for the three MCS lines. Figure 19 displays the restored seismic lines along with their finite elongation values of 11.8% for CT1-8ab (eastern line, Fig. 19A), 16.7% for CT1-6ab (central line, Fig. 19B) and 21.3% for CT1-3 (western line, Fig. 19C). These values support the prediction of progressive east to west increase in extension indicated by the instantaneous GPS-based strain calculations (Fig. 18).

We make a second estimate of extension across the Honduras borderlands by extrapolating the instantaneous GPS-based Caribbean plate vector (Fig. 18) to 12 Ma (the late Miocene age of initiation of rift based on well data). Assuming full strain partitioning, 24.7% extension occurred across the 150-km-wide Honduran borderlands at longitude 85°W (roughly the location of line CT1-3ab and CT1-6ab) (Fig. 19D). While these numbers are very close, the smaller extension values (11.8%–21.3%) obtained by the restoration of seismic lines compared to the GPS-based estimate (24.7%) may be the result of (1) incomplete partitioning (i.e., more motion on strike-slip faulting of the Swan Islands fault zone or on strike-slip faults within the rifts and basement ridges); (2) extension south of the region covered by the seismic lines; and (3) that the trend of the seismic lines are somewhat oblique rather than perpendicular to the trend of faults (Fig. 2A). Our analyses are consistent with Miocene age north-south extension determined from a paleostress analysis on striated fault planes from outcrops on Roatan Island, the largest of the Bay Islands, by Avé Lallemant and Gordon (1999).

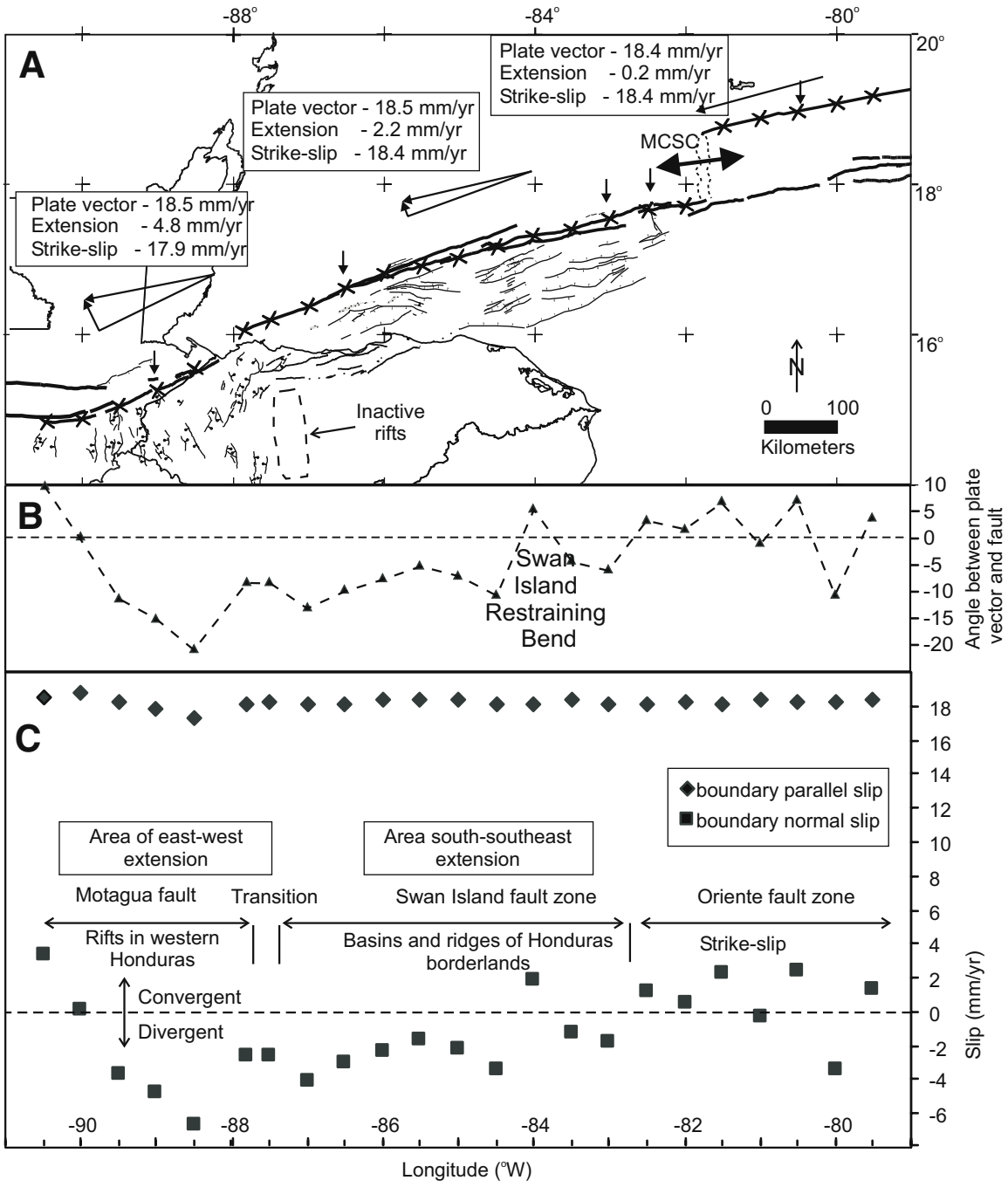

Figure 18. (A) Distribution of active faults along and south of the North America–Caribbean plate margin. GPS-derived Caribbean plate velocity (DeMets et al., 2000) was calculated at 30 min increments (Xs on map) along the main North America–Caribbean plate boundary faults (Motagua–Swan Islands–Mid-Cayman spreading center–Oriente system). The three plate vectors shown are for points along the fault system at longitudes 89°W, 85°W, and 81°W and are decomposed to show the extensional and strike-slip component of the plate vector. The extensional component of motion is controlled by the angular divergence between the plate vector and the trend of the plate boundary fault. Vertical arrows show location North America–Caribbean velocity predictions of DeMets et al. (2000). (B) Plot of the angular difference between the North America–Caribbean GPS-derived plate vector from DeMets et al. (2000) and the trend of the Motagua–Swan Islands–Mid-Cayman spreading center–Oriente fault system taken at the points along the fault system marked by "X" in Figure 18A. An angle of 0° would indicate predicted pure strike-slip; angles above the dashed line indicate convergence as observed at the Swan Islands restraining bend, and angles below the dashed line indicate divergence. (C) Plot of the Caribbean velocity components decomposed into rates of plate-boundary parallel slip (diamonds) and boundary-perpendicular slip (squares). MCSC—Mid-Cayman spreading center.

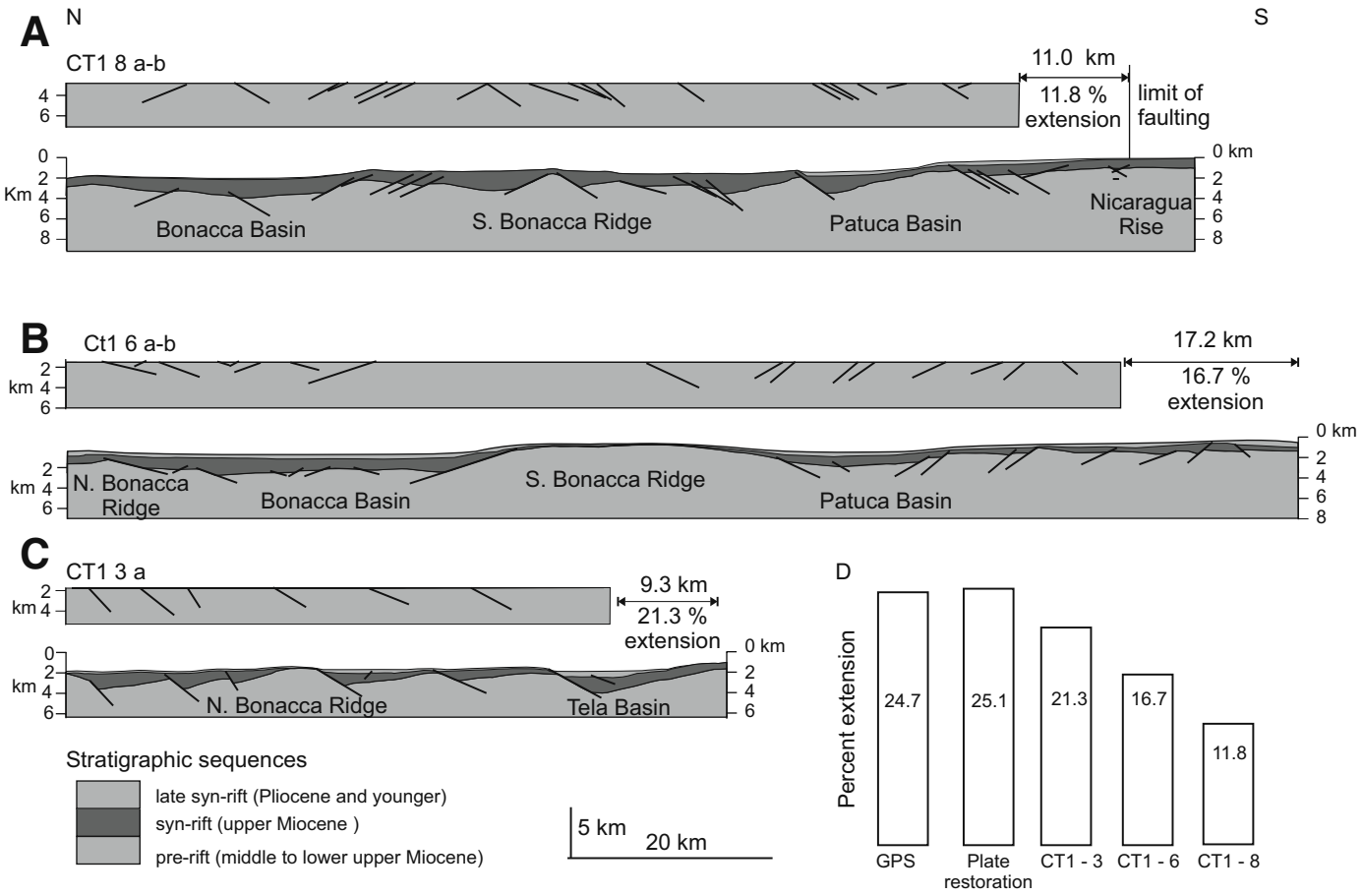

Figure 19. Interpretation of depth converted and restored University of Texas Institute for Geophysics multi-channel seismic (MCS) lines across the Honduran borderlands (cf. Fig. 2B for locations of three seismic lines). Interval velocities derived from well velocities in Honduran offshore exploration wells whose logs are shown in Figure 17 were used to convert time sections to depth sections (average velocity of pre-rift sequence 1:3.3 km/sec; syn-rift sequence 2:3.0 km/sec; late syn-rift sequence 3:2.2 km/sec). (A) Restoration of CT1-8ab MCS line restored to top of pre-rift sequence 1 yields 17.0 km or 18.3% extension compared to unrestored depth converted line. (B) Restoration of CT1-6ab MCS line restored to top of pre-rift sequence 1 yields 17.2 km or 16.7% extension compared to unrestored depth converted line. (C) Restoration of CT1-3ab MCS line restored to top of pre-rift sequence 1 yields 9.3 km or 21.3% extension compared to unrestored depth converted line. (D) Comparison of percent extension predicted from boundary normal slip (24.7%) known from present-day GPS measurements of the Caribbean plate (DeMets et al., 2000) with percent extension predicted from extrapolating the present-day GPS rate for the period of known rifting (25.1%) and with percent extension measured on the three seismic lines.

A third estimate of extension across the borderland is a byproduct of plate reconstruction that utilizes variable rates of Caribbean plate motion during the past 12 m.y. rather than extrapolation of the instantaneous GPS-derived plate motion vector. The extension calculated from the plate reconstruction process shows 25.1% extension across the Honduran borderlands (Fig. 19D), which is consistent with the other estimates of extension.

We make two estimates of extension across the 340-km-wide zone of north-trending rifts of Honduras and Guatemala (centered on longitude 89°W) using (1) the instantaneous GPS-derived plate motion vector and (2) the cumulative plate restoration process. The GPS-based method resulted in 45.0 km or 15.3% extension for the past 12 m.y. This is in close agreement with the extension estimate obtained through the plate restoration process, which yields an extensional amount of 47.8 km, or 16.3% extension.

Plate Reconstructions of Transtensional Environments in the Northwestern Caribbean

In order to address the question of how the features of the northwest corner of the Caribbean plate have evolved, we utilize quantitative plate restorations. In Figure 20, we present six quantitative plate reconstructions made to illustrate the complex evolution of this transtensional plate margin segment for the past 20 m.y. (early Miocene). The position of the North America plate is

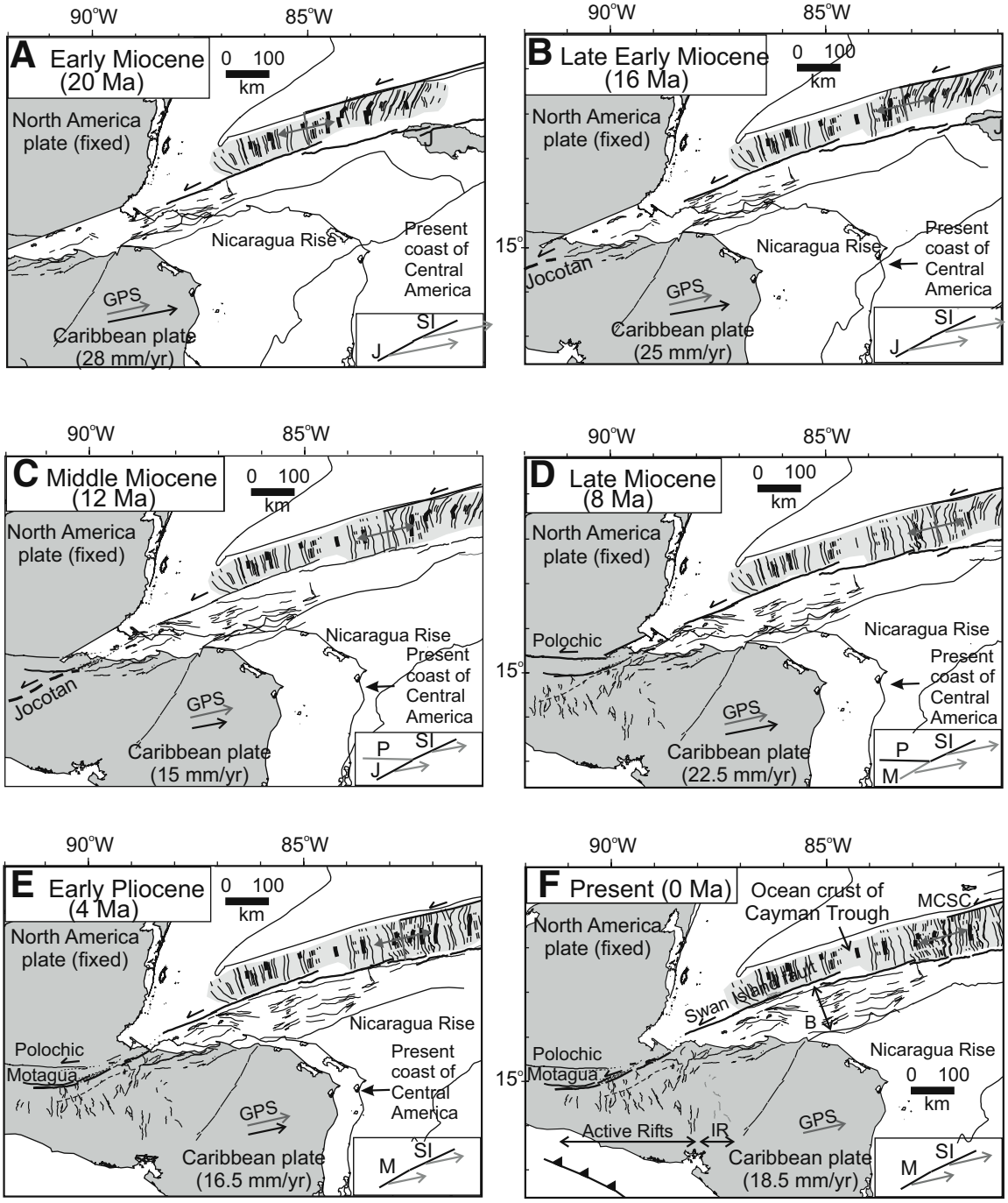

Figure 20. Plate tectonic reconstructions of northern Central America, the Cayman trough, and the Honduran borderlands with the North America plate held fixed. Plate boundary faults (P—Polochic fault; M—Motagua fault; SI—Swan Islands fault) are held fixed to the North America plate with the exception of the Jocatan (J) fault. Rotations are based on interpretations of ages of Cayman trough magnetic anomalies formed at Mid-Cayman spreading center (MCSC) by Rosencrantz (1994). Arrows show the direction and rate of the GPS present-day motion of the Caribbean plate from DeMets et al. (2000) compared to the predicted rate of past Caribbean plate motion from the Rosencrantz (1994) anomaly interpretation. Inset box summarizes the direction of the Rosencrantz (1994) direction of Caribbean plate motion relative to the plate boundary faults system inferred to have been active during that time period based on previous geologic studies by summarized by Burkart (1994) and Donnelly et al. (1990). (A) Early Miocene (20 Ma): The Jocotan–Swan Islands fault system is active. (B) Late early Miocene (16 Ma): The Jocotan–Swan Islands fault system is active. (C) Middle Miocene (12 Ma): The Jocotan–Swan Islands fault system is active. (D) Late Miocene (8 Ma): The Polochic–Swan Islands fault system is active. (E) Early Pliocene (4 Ma): The Polochic–Swan Islands fault system is active. (F) Present-day (0 Ma): The Motagua–Swan Islands fault system is active. Note that the present day coast of Central America is shown to provide an indication of cumulative lateral offset between the two plates. IR—inactive rifts.

fixed and the present-day coastline of Central America is shown in all the reconstructions as a frame of reference. Two vectors are shown on each reconstruction: (1) the current GPS-derived Caribbean plate motion vector (DeMets et al., 2000), and (2) the plate vector derived from magnetic anomalies in the surrounding oceanic basins, including the Cayman trough (Rosencrantz, 1994). Reconstruction results in a 20 m.y. average Caribbean plate vector of 21.4 mm/yr at azimuth N78E relative to North America. That is slightly greater than the 18.5 mm/yr at azimuth N77E GPS measured rate at 15°N, 85°W. A small inset map at the bottom of each reconstruction summarizes the major faults that are known from geologic studies to be active during that time interval along with the angle between these faults and the magnetic anomaly–derived plate vector inferred for that time period.

In the late early Miocene (16 Ma) and early Miocene (20 Ma) the Jocotan fault was the main plate boundary fault (Ritchie, 1976) (Figs. 20A and 20B). Our reconstruction suggests that the Jocotan fault formed a much straighter continuation of the Swan Islands fault than either the Polochic or Motagua would at a later time. This alignment places the Chamelecon and the La Ceiba fault in a position to be part of the plate boundary fault. No evidence for the north-trending rifts of the western area is known from this time. However, it is possible that borderland-style deformation "rifts parallel to margin" may have extended south of the plate margin because the geometry between the bounding fault and the plate motion vector is similar to that of today.

In the middle Miocene (12 Ma), the Jocotan fault was still the main plate boundary fault (Ritchie, 1976) (Fig. 20C). A major middle Miocene unconformity occurs in the Honduran borderland between deformed basement to Eocene rocks and overlying middle Miocene shallow-water clastic sedimentary rocks (Fig. 18). Subsidence in the Honduran borderland region is evidenced by deposition of the pre-rift sequence and may indicate the onset of transtension in this region.

By the late Miocene (8 Ma), the plate boundary shifted to the north and the Polochic fault was active (Burkart, 1983) (Fig. 20D). The north-south–trending rifting in western Honduras commenced shortly before this prior time (after 10.5 Ma according to Gordon and Muehlberger, 1994). We suggest that north-south rifts of the western area were initiated by the plate boundary moving from the Jocotan to the Polochic fault, thereby increasing the divergence between the Caribbean plate motion vector and the plate margin fault. According to the offshore wells, the late Miocene is the when the rift basins of the Honduran borderlands were filling with syn-rift sediments (Fig. 12).

During the early Pliocene (4 Ma), the plate margin fault geometry (Fig. 20E) remained the same as in the late Miocene. In the Honduran borderlands, well and seismic data indicates that the rift phase that began in the late Miocene is ongoing. According to Burkart (1983), the plate boundary shifted from the Polochic fault to the Motagua fault shortly after this time. This switch to the arcuate Motagua fault increased the angle of divergence and amount of strain partitioning in the area of north-south rifting.

At present, the main left-lateral faults of the plate boundary zone are the Motagua (Plafker, 1976) and Swan Islands fault zone (Rosencrantz and Mann, 1991) (Fig. 20F). The Polochic fault in Guatemala, although active, is no longer the plate boundary. Rifting of the Honduran borderlands is decreasing (seismic sequence 3 in Fig. 12). This decrease in rifting may be related to the eastward movement of this area into an area of lesser plate divergence. A zone of inactive, north-trending rifts exists in east-central Honduras (IR in Fig. 20F). These rifts were generated west of their present position and rafted eastward with the Caribbean plate.

CONCLUSIONS

The main conclusions of this study are as follows:

1. Geologic, earthquake, marine geophysical, and remote sensing data from on- and offshore areas show that Neogene to Recent transtensional deformation along the North America–Caribbean plate boundary in northern Central America exhibits two distinct structural styles. In the western area, east-west extension affects a 375-km-long plate boundary segment with basin and range morphology in western Honduras and northern Guatemala. In the eastern study area, NNW-SSE transtension occurs along a 600-km-long plate boundary segment of margin-parallel ridges and basins in the Nombre de Dios range and Aguan Valley of northern Honduras and offshore Honduran borderlands region (Fig. 2).
2. Comparison of fault orientations and the trend of the GPS-derived Caribbean plate motion vector show that east-west extension along faults normal to the plate boundary occurs in the western area when the angle of divergence between the Motagua plate boundary fault and the plate motion vector is ≥10° (Fig. 18). This oblique opening model differs from previous interpretations of Burkart and Self (1985) that invoke block rotations about the arcuate Motagua fault zone.
3. In northern Honduras and its borderland, NNW-SSE extension along faults subparallel to the plate margin coincide with an angle between the Swan Islands plate bounding fault and the plate motion vector of between 5 and 10°.
4. A narrow, 35-km-wide tectonic transition area in north-central Honduras separates the north-trending rifts of western Honduras from the plate boundary–parallel rifts in northeastern Honduras and the offshore Honduran borderlands (Fig. 2).
5. Faults of the offshore Honduran borderlands extend onshore into the Nombre de Dios range and Aguan Valley of northern Honduras, where subaerial transtensional deformation is similar to deformation of the submarine Honduran borderlands (Fig. 5). Tectonic geomorphology studies show pervasive oblique-slip faulting with evidence for late Quaternary left-lateral offsets (Fig. 7) and active uplift of stream networks (Fig. 6).

6. Seismic data tied to wells in the Honduran borderlands (Fig. 18) show that plate boundary–related submarine faults in this region are active, transtensional features that initiated in the middle Miocene with filling of asymmetric half-grabens and continued through the Pliocene-Pleistocene.
7. Quantitative plate reconstructions suggest that the north-trending rifts of the western region developed in response to increased interplate divergence as the plate boundary shifted from the Jocotan fault to the Polochic fault prior to 8 Ma.

ACKNOWLEDGMENTS

Funding for R. Rogers and P. Mann was provided by the Petroleum Research Fund of the American Chemical Society (grant 33935-AC2 to P. Mann). We thank Dirección de Energia of Honduras and Japanese Petroleum Exploration Co. Geoscience Institute for releasing data for this study. P. Emmet, M. Gordon, and C. DeMets provided comments on an earlier version of the manuscript. We thank J. Marshall, T. Wawrzyniec, and M. Guzman-Speziale for their reviews. Lisa Gahagan at Institute for Geophysics provided plate reconstructions. This is University of Texas Institute for Geophysics contribution no. 1869.

REFERENCES CITED

Avé Lallemant, H., and Gordon, M., 1999, Deformation history of Roatan Island: Implications for the origin of the Tela basin (Honduras), *in* Mann, P., ed., Caribbean basins, Sedimentary basins of the world series: Amsterdam, Elsevier, v. 4, p. 197–218.

Ben-Avraham, Z., 1992, Development of asymmetric basins along continental transform margins: Tectonophysics, v. 215, p. 209–220, doi: 10.1016/0040-1951(92)90082-H.

Ben-Avraham, Z., and Zoback, M., 1992, Transform-normal extension and asymmetric basins: An alternative to pull-apart models: Geology, v. 20, p. 423–426, doi: 10.1130/0091-7613(1992)020<0423:TNEAAB>2.3.CO;2.

Burkart, B., 1983, Neogene North America–Caribbean plate boundary across northern Central America: Offset along the Polochic fault: Tectonophysics, v. 99, p. 251–270, doi: 10.1016/0040-1951(83)90107-5.

Burkart, B., 1994, Northern Central America, *in* Donovan, S., and Jackson, T., eds., Caribbean geology: An introduction: Jamaica, University of the West Indies Publisher's Association, p. 265–284.

Burkart, B., and Self, S., 1985, Extension and rotation of crustal blocks in northern Central America and effect on the volcanic arc: Geology, v. 13, p. 22–26, doi: 10.1130/0091-7613(1985)13<22:EAROCB>2.0.CO;2.

Cáceres, D., Monterroso, D., and Tavakoli, B., 2005, Crustal deformation in northern Central America: Tectonophysics, v. 404, p. 119–131, doi: 10.1016/j.tecto.2005.05.008.

Calais, E., and Mercier de Lépinay, B., 1993, Semiquantitative modeling of strain and kinematics along the Caribbean–North America strike-slip plate boundary zone: Journal of Geophysical Research, v. 98, p. 8293–8308.

Calais, E., Mazabraud, Y., Mercier de Lépinay, B., Mann, P., Jansma, P., and Mattioli, G., 2002, Oblique collision and strain partitioning from GPS measurements in the northeastern Caribbean: Geophysical Research Letters, v. 29, no. 18, p. 3-1–3-4.

Case, J., and Holcombe, T., 1980, Geologic-tectonic map of the Caribbean region: U.S. Geological Survey Miscellaneous Investigations Series I-1100, scale 1:2,500,000.

Claypool, A., Klepeis, K., Dockrill, B., Clarke, G., Zwingmann, H., and Tulloch, A., 2002, Structure and kinematics of oblique continental convergence in northern Fiordland, New Zealand: Tectonophysics, v. 359, p. 329–358, doi: 10.1016/S0040-1951(02)00532-2.

Deng, J., and Sykes, L., 1995, Determination of Euler pole for contemporary relative motion of Caribbean and North American plates using slip vectors of interplate earthquakes: Tectonics, v. 14, p. 39–53, doi: 10.1029/94TC02547.

DeMets, C., Jansma, P., Mattioli, G., Dixon, T., Farina, F., Bilham, R., Calais, E., and Mann, P., 2000, GPS geodetic constraints on Caribbean-North American plate motion: Geophysical Research Letters, v. 27, p. 437–440, doi: 10.1029/1999GL005436.

Donnelly, T., Horne, G., Finch, R., and López-Ramos, E., 1990, Northern Central America: The Maya and Chortis blocks, *in* Dengo, G., and Case, J., eds., The Caribbean region: Geological Society of America, Geology of North America, v. H, p. 37–76.

Dupré, W.R., 1970, Geology of the Zambrano Quadrangle, Honduras, Central America [M.A. thesis]: Austin, Texas, University of Texas at Austin, 128 p.

ENEE (Empressa Nacional de Energia Electrica), 1987, Geologic investigations of proposed hydrothermal sites, Honduras: Tegucigalpa, Honduras, Honduras Electrical Company unpublished report, 24 p.

Everett, J., 1970, Geology of the Comayagua Quadrangle, Honduras, Central America [Ph.D. dissertation]: Austin, Texas, University of Texas at Austin, 152 p.

Gardner, T., Back, W., Bullard, T., Hare, P., Kesel, R., Lowe, D., Menges, C., Mora, S., Pazzaglia, F., Sasowsky, I., Troester, J., and Wells, S., 1987, Central America and the Caribbean, *in* Graf, W., ed., Geomorphic systems of North America: Boulder, Colorado, Geological Society of America Centennial Special Volume, v. 2, p. 343–402.

Gordon, M., 1994, Evolution of Neogene microtectonic phases on the Chortís block (Northern Central America): Geological Society of America Abstracts with Programs, v. 26, no. 7, p. A-209.

Gordon, M., and Muehlberger, W., 1994, Rotation of the Chortís block causes dextral slip on the Guayape fault: Tectonics, v. 13, p. 858–872, doi: 10.1029/94TC00923.

Gorsline, D.S., and Teng, L.S.-Y., 1989, The California continental borderland, *in* Winterer, E.L., Hussong, D.M., and Decker, R.W., eds., The Eastern Pacific Ocean and Hawaii: Boulder, Colorado, Geological Society of America, Geology of North America, v. N, p. 471–487.

Guzman-Speziale, M., 2001, Active seismic deformation in the grabens of northern Central America and its relationship to the relative motion of the North America–Caribbean plate boundary: Tectonophysics, v. 337, p. 39–51, doi: 10.1016/S0040-1951(01)00110-X.

Hack, J., 1957, Studies of longitudinal stream profiles in Virginia and Maryland: U.S. Geological Survey Professional Paper 294B, p. 45–97.

Helbig, K., 1959, Die landschaften von Nordost—Honduras: Petermanns Geographischen Mitteilungen, Veb Hermann Haack, Geographisch-Kartographische Anstalt, Gotha, Ergänzungsheft Nr. 268, 270 p.

Hovius, N., 2000, Macroscale process systems of mountain belt erosion, *in* Summerfield, M., ed., Geomorphology and global tectonics: Chichester, UK, John Wiley & Sons, p. 77–105.

Jansma, P., Lopez, A., Mattioli, G., DeMets, C., Dixon, T., Mann, P., and Calais, E., 2000, Neotectonics of Puerto Rico and the Virgin Islands, northeastern Caribbean, from GPS geodesy: Tectonics, v. 19, p. 1021–1037, doi: 10.1029/1999TC001170.

Jones, R., and Tanner, P., 1995, Strain partitioning in transpression zones: Journal of Structural Geology, v. 17, p. 793–802, doi: 10.1016/0191-8141(94)00102-6.

Jordan, B.R., Sigurdsson, H., Carey, S., Lundin, S., Rogers, R., and Barquero-Molina, M., 2007, this volume, Petrogenesis of Central American Tertiary ignimbrites and associated Caribbean Sea tephra, *in* Mann, P., ed., Geologic and tectonic development of the Caribbean margin in northern Central America: Geological Society of America Special Paper 428, doi: 10.1130/2007.2428(07).

Kanamori, H., and Stewart, G., 1978, Seismological aspects of the Guatemala earthquake of February 4, 1976: Journal of Geophysical Research, v. 83, p. 3427–3434.

King, A., 1972, Mapa Geológica de Honduras, Hoja de Talanga (Geologic Map of Honduras, Talanga sheet): Tegucigalpa, Honduras, Instituto Geográfico Nacional, 1 sheet, scale 1:50,000.

King, A., 1973, Mapa Geológica de Honduras, Hoja de Cedros (Geologic Map of Honduras, Cedros sheet): Tegucigalpa, Honduras, Instituto Geográfico Nacional, scale, 1:50,000.

Kornicker, L., and Bryant, W., 1969, Sedimentation on continental shelf of Guatemala and Honduras, Tectonic relations of northern Central America

and the western Caribbean—The Bonacca Expedition: American Association of Petroleum Geologists Memoir 11, p. 244–257.

Kozuch, M., 1991, Mapa Geológica de Honduras: Tegucigalpa, Honduras, Instituto Geográfico Nacional, 3 sheets, scale 1:500,000.

Langer, C., and Bollinger, G., 1979, Secondary faulting near the terminus of a seismogenic strike-slip fault; aftershocks of the 1976 Guatemala earthquake: Bulletin of the Seismological Society of America, v. 69, p. 427–444.

Leeder, M., and Alexander, J., 1987, The origin and tectonic significance of asymmetrical meander-belts: Sedimentology, v. 34, p. 217–226, doi: 10.1111/j.1365-3091.1987.tb00772.x.

Leroy, S., Mauffret, A., Patriat, P., and Mercier de Lepinay, B., 2000, An alternative interpretation of the Cayman Trough evolution from a reidentification of magnetic anomalies: Geophysical Journal International, v. 141, p. 539–557, doi: 10.1046/j.1365-246x.2000.00059.x.

Mann, P., and Burke, K., 1984, Neotectonics of the Caribbean: Reviews of Geophysics and Space Physics, v. 22, p. 309–362.

Mann, P., Tyburski, S., and Rosencrantz, E., 1991, Neogene development of the Swan Islands restraining bend complex, Caribbean Sea: Geology, v. 19, p. 823–826, doi: 10.1130/0091-7613(1991)019<0823:NDOTSI>2.3.CO;2.

Mann, P., Calais, E., Ruegg, J., DeMets, C., Dixon, T., Jansma, P., and Mattioli, G., 2002, Oblique collision in the northeastern Caribbean from GPS measurements and geological observations: Tectonics, v. 21, 1057, doi: 10.1029/2001TC001304.

Manton, W., 1987, Tectonic interpretation of the morphology of Honduras: Tectonics, v. 6, p. 633–651.

Manton, W., and Manton, R., 1999, The southern flank of the Tela basin, Republic of Honduras, *in* Mann, P., ed., Caribbean basins: Sedimentary basins of the world series: Amsterdam, Elsevier, v. 4, p. 219–236.

Marshall, J., Fisher, D., and Gardner, T., 2000, Central Costa Rica deformed belt; kinematics of diffuse faulting across the western Panama Block: Tectonics, v. 19, p. 468–492, doi: 10.1029/1999TC001136.

Markey, R., 1995, Mapa Geológica de Honduras, Hoja de Morocelli (Geologic Map of Honduras, Morocelli sheet): Tegucigalpa, Honduras, Instituto Geográfico Nacional, 1 sheet, scale 1:50,000.

Meckel, T., Coffin, M., Mosher, S., Symonds, P., Bernard, G., and Mann, P., 2003, Underthrusting at the Hjort Trench, Australian-Pacific plate boundary: Incipient subduction? Geochemistry, Geophysics, Geosystems, v. 4, no. 12, 1099, doi: 10.1029/2002GC000498.

Molnar, P., and Sykes, L., 1969, Tectonics of the Caribbean and Middle America regions from focal mechanisms and seismicity: Geological Society of America Bulletin, v. 80, p. 1639–1684.

Muehlberger, W., 1976, The Honduras Depression: Publicaciones Geológicas del ICAITI (Guatemala): Issue 5, p. 43–51.

Pinet, P., 1971, Structural configuration of the northwestern Caribbean plate boundary: Geological Society of America Bulletin, v. 82, p. 2027–2032.

Pinet, P., 1972, Diapirlike features offshore Honduras: Implications regarding tectonic evolution of Cayman Trough and Central America: Geological Society of America Bulletin, v. 83, p. 1911–1922.

Pinet, P., 1975, Structural evolution of the Honduras continental margin and the sea floor south of the western Cayman Trough: Geological Society of America Bulletin, v. 86, p. 830–838, doi: 10.1130/0016-7606(1975)86<830:SEOTHC>2.0.CO;2.

Pinet, P., 1976, Morphology off northern Honduras, northwest Caribbean Sea: Deep Sea Research, v. 23, p. 839–847.

Plafker, G., 1976, Tectonic aspects of the Guatemala earthquake of 4 February, 1976: Science, v. 193, p. 1201–1208, doi: 10.1126/science.193.4259.1201.

Ritchie, A., 1976, Jocotan Fault; possible western extension: Publicaciones Geológicas del ICAITI (Guatemala): Issue 5, p. 52–55.

Rogers, R., 1995, Mapa Geológica de Honduras, Hoja de Valle de Jamastran (Geologic Map of Honduras, Valle de Jamastran sheet): Tegucigalpa, Honduras, Instituto Geográfico Nacional, 1 sheet, scale 1:50,000.

Rogers, R., and O'Conner, E., 1993, Mapa Geológica de Honduras: Hoja de Tegucigalpa (segunda edición): Tegucigalpa, Honduras, Instituto Geográfico Nacional, 1 sheet, scale 1:50,000.

Rogers, R., Kárason, H., and van der Hilst, R., 2002, Epeirogenic uplift above a detached slab in northern Central America: Geology, v. 30, p. 1031–1034, doi: 10.1130/0091-7613(2002)030<1031:EUAADS>2.0.CO;2.

Rogers, R.D., Mann, P., Emmet, P.A., and Venable, M.A., 2007, this volume, Colon fold belt of Honduras: Evidence for late Cretaceous collision between the continental Chortis block and intraoceanic Caribbean arc, *in* Mann, P., ed., Geologic and tectonic development of the Caribbean margin in northern Central America: Geological Society of America Special Paper 428, doi: 10.1130/2007.2428(06)

Rogers, R.D., Mann, P., Scott, R., and Patino, L., 2007, this volume, Cretaceous intra-arc rifting, sedimentation and basin inversion in east-central Honduras, *in* Mann, P., ed., Geologic and tectonic development of the Caribbean margin in northern Central America: Geological Society of America Special Paper 428, doi: 10.1130/2007.2428(05).

Rosencrantz, E., 1994, Opening of the Cayman Trough and the evolution of the northern Caribbean Plate boundary: Geological Society of America Abstracts with Programs, v. 27, no. 7, p. A-59.

Rosencrantz, E., and Mann, P., 1991, SeaMarc II mapping of transform faults in the Cayman Trough, Caribbean Sea: Geology, v. 19, p. 690–693, doi: 10.1130/0091-7613(1991)019<0690:SIMOTF>2.3.CO;2.

Rowan, M., and Kligfield, R., 1989, Cross-section restoration and balancing as aid to seismic interpretation in extensional terranes: AAPG Bulletin, v. 73, p. 955–966.

Sandwell, D., and Smith, W., 1997, Marine gravity anomaly from Geosat and ERS-1 satellite altimetry: Journal of Geophysical Research, v. 102, p. 10,039–10,054, doi: 10.1029/96JB03223.

Schwartz, D., Cluff, L., and Donnelly, T., 1979, Quaternary faulting along the Caribbean–North American plate boundary in Central America: Tectonophysics, v. 52, p. 431–445, doi: 10.1016/0040-1951(79)90258-0.

Sigurdsson, H., Kelley, S., Leckie, R., Carey, S., Bralower, T., and King, J., 2000 History of circum-Caribbean explosive volcanism: $^{40}Ar/^{39}Ar$ dating of tephra layers, *in* Leckie, R., and Sigurdsson, H., et al., eds., Proceedings of the Ocean Drilling Program, Scientific Results, Leg 165: College Station, Texas, Ocean Drilling Program, v. 165, p. 299–314.

Smith, W., and Sandwell, D., 1997, Global seafloor topography from satellite altimetry and ship depth soundings: Science, v. 277, p. 1957–1962.

Teyssier, C., Tykoff, B., and Markley, M., 1995, Oblique plate motion and continental tectonics: Geology, v. 23, p. 447–450, doi: 10.1130/0091-7613(1995)023<0447:OPMACT>2.3.CO;2.

Van Dusen, S., and Doser, D., 2000, Faulting processes of historic (1917–1962) M> or = 6.0 earthquakes along the north-central Caribbean Margin: Pure and Applied Geophysics, v. 157, p. 719–736, doi: 10.1007/PL00001115.

Wadge, G., and Wooden, J.L., 1982, Late Cenozoic alkaline volcanism in the northwestern Caribbean: Tectonic setting and Sr isotopic characteristics: Earth and Planetary Science Letters, v. 57, p. 35–46, doi: 10.1016/0012-821X(82)90171-6.

Webb, D.S., and Perrigo, S.C., 1984, Late Cenozoic vertebrates from Honduras and El Salvador: Journal of Vertebrate Paleontology, v. 4, p. 237–254.

Manuscript Accepted by the Society 22 December 2006